CRYSTAL GROWTH & DESIGN

Review

pubs.acs.org/crystal

Enhancing Mixed-Matrix Membrane Performance with Metal–Organic Framework Additives

Janina Dechnik,[†] Christopher J. Sumby,*[,‡] and Christoph Janiak*[,†]

[†]Institut für Anorganische Chemie und Strukturchemie, Universität Düsseldorf, 40204 Düsseldorf, Germany

[‡]Department of Chemistry and the Centre for Advanced Nanomaterials, University of Adelaide, Adelaide, Australia

Supporting Information

ABSTRACT: Metal–organic frameworks (MOFs), as porous fillers possessing molecular sieving properties, have been combined with polymers to give mixed-matrix membranes (MMMs) with enhanced separation performance. This field of research has produced a large number of different membranes, and many MOF/polymer combinations have been tested and reported to show potential application to industrial gas separation. Although MOFs have been proposed as novel additives with high porosity and tunable pore size, which were supposed to outperform other porous fillers, due to restrictions in separation performance of the filler and challenges concerning the compatibility of polymer and MOF, only a small fraction of these works report both improved permeability and selectivity. In this review these challenges are set into the context of MOF synthesis and membrane fabrication by the choice of appropriate polymer/MOF combinations, utilization of the MOF functional sites, modification of the MOF surface chemistry or pore texture and size, and also targeted influence of the size and shape of the filler particles. The effect of the highlighted MOF additives on the gas separation performance is analyzed and discussed by comparison of the gas permeability and selectivity. This emphasizes strategies by which high performing MMMs can be achieved through accessing the full potential of the porous MOF fillers.

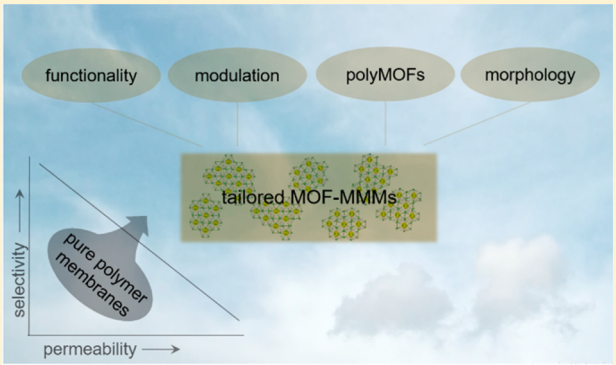

1. INTRODUCTION

Artificial membranes are frequently used in chemical industrial processes. Membranes are thin layers that provide a resistance to the passage of different substances. Theoretically they can be used in any process for the separation of substances. Gas purification, the production of drinking water from seawater (water desalination), the purification of sewage, and the recovery of fuel vapors are some of the most important examples of membrane applications.[1]

Membrane separation processes are very versatile and are specified by their application demand, i.e., in industrial processes, or in the production of purified substances. The specification of which kind of membrane material or process is applied depends on the given separation problem and the conditions like feed composition, compression of feed streams, or contamination by substances which influence the separation process. The process or membrane material that is to be chosen for a specific separation problem is mainly determined by the size of the components of the mixture. Research into the development of new membrane materials mostly focuses on the development of dense polymer membranes where the effect of modifications is also studied compared to the pure or unmodified polymer material. Such membranes are characterized for gas separations because of the very similar size of the substances and the demand for industrial application.

Industrial separation processes are commonly carried out with conventional methods, such as distillation, crystallization, or absorption. The use of membrane separation processes often proves to be more advantageous than these methods for many applications. Particularly the lower costs, the lower energy consumption, and simpler process conditions make membrane separation processes the preferred technology for the purification of mixtures.[2] Membrane separation processes can give energy savings of up to 50% of the production cost over other separation technologies.[3,4] Membrane processes, which are already in place in industry, include the removal of CO_2 from natural gas (before the natural gas can be passed to the pipeline), the isolation and recovery of hydrogen (for example in cracking processes), and oxygen/nitrogen separation from air (for enriched oxygen in medical devices and enriched nitrogen used for oxygen sensitive materials).[2,5] Membrane processes for vapor[6] or monomer recovery, e.g., ethylene/N_2 or propylene/N_2 separation,[7,8] or for the removal of water or larger molecules from organic solvents[9] are increasingly applied. Organic polymers are typically used for commercial membranes as they are inexpensive and easy to manufacture.

Received: April 25, 2017
Published: June 12, 2017

DOI: 10.1021/acs.cgd.7b00595
Cryst. Growth Des. 2017, 17, 4467–4488

Table 1. Permeability and Selectivity Data of the Highlighted MMMs and Corresponding Polymer Membranes[a]

			P^b [Barrer]	selectivity		Measurement conditions[d]			
filler (specification)	polymer	filler-ldg. [wt %]	CO_2	CO_2/CH_4	CO_2/N_2[c]	T [°C]	Δp [bar]	method	ref
	PSF	0	7	27		30	10	mixed sweep	107
NH_2-MIL-125(Ti)		10	15	29					
		20	23	30					
		30	37	6					
	Matrimid 9725	0	6	30		35	9	mixed const vol.	108
MIL-125(Ti)		15	18	44					
		30	27	37					
NH_2-MIL-125(Ti)		15	17	50					
		30	50	37					
	SPEEK	0	16	23	34	30	1.5	single sweep, dry	111
MIL-101(Cr)		40	31	31	37				
HSO_3-MIL-101(Cr)		40	35	40	41				
	SPEEK	0	543[h]	23[h]	34[h]	30	1.5	single sweep, humid	
MIL-101(Cr)		40	1623	33	40				
HSO_3-MIL-101(Cr)		40	2064	50	53				
	SPEEK	0	16[h]	22[h]	33[h]	30	1.5	mixed sweep, dry, CO_2/CH_4 (30/70) CO_2/N_2 (20/80)	
MIL-101(Cr)		40	29	29	36				
HSO_3-MIL-101(Cr)		40	34	39	40				
	SPEEK	0	540[h]	21[h]	32[h]	30	1.5	mixed sweep, humid CO_2/CH_4 (30/70), CO_2/N_2 (20/80)	
MIL-101(Cr)		40	1600[h]	31[h]					
		40	1609[h]		39[h]				
HSO_3-MIL-101(Cr)		40	2029[h]	48[h]					
		40	2013[h]		51[h]				
	Matrimid 9725	0	6	31		35	9	mixed const. vol.	129
UiO-66(Zr)		30	16	36					
UiO-66(Zr)-BA		30	18	43					
UiO-66(Zr)-ABA		30	14	45					
NH_2-UiO(Zr)-66		30	18	37					
NH_2-UiO-66(Zr)-BA		30	17	39					
NH_2-UiO-66(Zr)-ABA		30	38	48					
	PSF asymm.	0	204	21		30	6	mixed sweep	136
ZIF-8		6	420	19					
IL@ZIF-8		6	312	34					
		0	227		26				
ZIF-8		6	464		29				
IL@ZIF-8		6	351		115				
	PMMA	0	(O_2) 0.09		(O_2/N_2) 8	35	2	single const. vol.	140
	PMMA	0	(O_2) 0.09		(O_2/N_2) 8	35	2	single const. vol.	141
		0	(O_2) 0.11		(O_2/N_2) 8				
NH_2-CAU-1		15	(O_2) 633		(O_2/N_2) 2	25	1	single const. vol.	139
NH_2-CAU-1@PDA		15	(O_2) 627		(O_2/N_2) 3				
	Matrimid 5218	0	8		29	25	n.s.	single const. vol.	123
NH_2-UiO-66		23	23[h]		35[h]				
NH_2-UiO-66-PA		23	28[h]		36[h]				
NH_2-UiO-66-C10		23	22[h]		27[h]				
NH_2-UiO-66-SA		23	19[h]		30[h]				
	SPEEK	0	15[h]	27[h]	37[h]	30	1.5	single sweep, dry	143
MIL-101(Cr)		40	29	32	39				
PEI@MIL-101(Cr)		40	36	40	48				
	SPEEK	0	545	25	36	30	1.5	single sweep, humid	
MIL-101(Cr)		40	1623	32	40				
PEI@MIL-101(Cr)		40	2490	72	80				
MIL-101(Cr)		40	29	32	38	30	1	mixed sweep, dry CO_2/CH_4 (30/70), CO_2/N_2 (10/90)	143

DOI: 10.1021/acs.cgd.7b00595
Cryst. Growth Des. 2017, 17, 4467−4488

Table 1. continued

filler (specification)	polymer	filler-ldg. [wt %]	P^b [Barrer] CO_2	selectivity CO_2/CH_4	selectivity CO_2/N_2[c]	Measurement conditions[d] T [°C]	Δp [bar]	method	ref
PEI@MIL-101(Cr)		40	36	39	47				
	SPEEK	0	529[h]	22[h]	33[h]	30	1	mixed sweep, humid CO_2/CH_4 (30/70), CO_2/N_2 (10/90)	
MIL-101(Cr)		40	1586	30					
		40	1548		38				
PEI@MIL-101(Cr)		40	2384	70					
		40	2437		78				
	6FDA–ODA	0	14[h]	50[h]		35	10	mixed const. vol.	53
MIL-53(Al)		25	21[h]	44[h]					
NH_2-MIL(Al)-53		10	14[h]	49[h]					
		15	14[h]	50[h]					
		20	14[h]	53[h]					
		25	14[h]	65[h]					
		30	15[h]	71[h]					
		32	15[h]	78[h]					
	6FDA–DAM	0	315	10		35	10	mixed const. vol.	171
MIL-53(Al)		10	330[h]	11[h]					
		15	351[h]	12[h]					
NH_2-MIL(Al)-53		10	307[h]	14[h]					
		15	288[h]	15[h]					
		20	298[h]	9[h]					
	6FDA–DAM–HAB	0	46[h]	34		35	10	mixed const. vol.	171
MIL-53(Al)		10	55[h]	37[h]					
		15	64[h]	41[h]					
NH_2-MIL(Al)-53		10	42[h]	78[h]					
		15	44[h]	65[h]					
		20	54[h]	35[h]					
	6FDA–DAM–HAB	0	54	18		35	10	single const. vol.	171
MIL-53(Al)		10	61	16					
		15	71	15					
NH_2-MIL(Al)-53		10	47	79					
		15	47	58					
		20	44	28					
	PVDF	0	0.9	21		25	6	mixed const. vol.	173
	m-PVDF	0	1.2	26					
MIL-53(Al)		5	1.8	35					
		10	2.5	37					
NH_2-MIL(Al)-53		5	1.7	37					
		10	2.2	43					
MIL-53(Al)-53	PVDF	5	1.2	21		25	6	mixed const. vol.	172
		10	1.6	21					
NH_2-MIL(Al)-53		5	1.1	23					
		10	1.4	26					
	Pebax 1657[e]	0	72	14	34	20	3.75	single const. press.	175
ZIF-7		8	145	23	68				
		22	111	30	97				
		34	41	44	105				
	Chitosan	0	307		0,5	50	2	single const. vol.	179
	Chitosan/ [emim][Ac]	0	1338		5				
ZIF-8		10	5413		12	50	2	single const. vol.	179
HKUST-1		5	4754		19				
	XLPEO	0	450	15		25	1	mixed sweep	195
bulk $Zn(pyrz)_2(SiF_6)$		10	540	23					
submicron Zn $(pyrz)_2(SiF_6)$		10	620	27					
		20	590	30					
	XLPEO	0	470		19	25	1	mixed sweep CO_2/N_2 (20/80)	195

DOI: 10.1021/acs.cgd.7b00595
Cryst. Growth Des. 2017, 17, 4467−4488

Table 1. continued

filler (specification)	polymer	filler-ldg. [wt %]	P^b [Barrer] CO_2	selectivity CO_2/CH_4	selectivity CO_2/N_2[c]	Measurement conditions[d] T [°C]	Δp [bar]	method	ref
bulk $Zn(pyrz)_2(SiF_6)$		10	540		25				
submicron $Zn(pyrz)_2(SiF_6)$		10	670		29				
		20	630		29				
	PBI	0	(H_2) 4		(H_2/CO_2) 10	35	5	single const. vol.	197
$(OH)_2$-UiO-66(Hf)		10	(H_2) 8		(H_2/CO_2) 19				
		20	(H_2) 11		(H_2/CO_2) 13				
		30	(H_2) 15		(H_2/CO_2) 8				
	Matrimid	0	8[h]	32[h]		35	5	mixed const. vol.	204
ZIF-8 (particle fusion)		30	26[h]	53[h]					
ZIF-8		30	20[h]	41[h]					
	PVC-*g*-POEM	0	70	14		35	1	single const. vol.	206
ZIF-8		10	170	12					
		20	495	11					
		30	623	11					

[a]The data were used to plot the comparative permselectivity graphs to visualize the impact of the different strategies to modify MMM materials for separation. [b]Permeability of preferentially permeating gas. If another gas other than CO_2 is the preferentially permeating gas, it is specified in brackets next to the value. [c]If another gas other than CO_2 is the preferentially permeating gas, the gas pair is specified in parentheses next to the value. [d]If not specified, in mixed gas experiments the feed gas composition is 50/50 vol %. [e]Composite membrane. [h]Data obtained and calculated from figures.

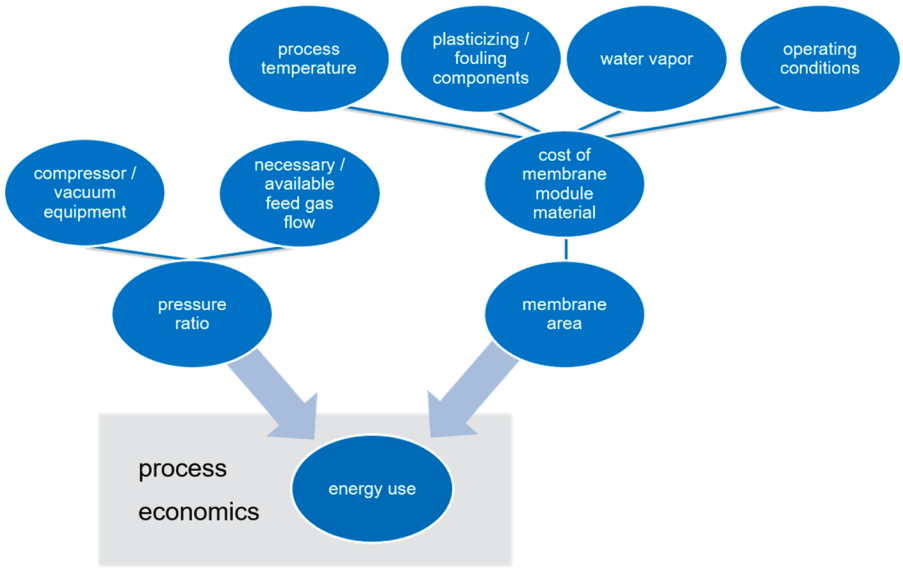

Figure 1. Factors that influence the process economics of a membrane gas separation process, in particular, energy use, and thereby determine the properties of the optimum membrane.

1.1. Membrane Performance Characteristics for Gas Separation. A brief mathematical description of permeability and selectivity is given in the Supporting Information.

The gas flow through the membrane is usually measured at "constant pressure and variable volume" or with "variable pressure and constant volume'". For mixed gas experiments a special sensor is used to determine the mole fractions of the components in gas streams. In the method to measure gas permeation with constant volume and variable pressure, the permeate flow is determined by detecting the pressure increase by a pressure transducer in a constant-volume cell in which permeate flows through the membrane.[10] For measurement approaches with "continuous flow" or "constant-pressure and variable-volume", direct measurement of the steady-state gas flow rate on the permeate side of a membrane is achieved using a flow meter. Commonly electronic flow meters or capillary soap-bubble flow meters are used for this purpose. Both methods can be used to directly measure the single gas permeability when pure gases are used as feed. If a gas mixture is applied as the feed gas, either the collected gas volume at steady state or a sample of the continuous flowing gas stream is directed to, for example, a gas chromatograph, to determine the permeate composition. Alternatively the permeating gas is

DOI: 10.1021/acs.cgd.7b00595
Cryst. Growth Des. 2017, 17, 4467−4488

directed from the membrane to the sensor system using a sweep gas stream at atmospheric pressure.

All above-mentioned methods are commonly used in studies on membrane gas separation performance (cf. Table 1), but in order to evaluate the practical separation performance of membranes, mixed-gas permeation tests should be performed. The mixed-gas permeability of membranes can be reduced, compared to their corresponding single gas permeabilities, due to the effect of permeate competition from the competitive sorption and diffusion of both gases.[11] Ideally a membrane should have both a high permeability and a high selectivity. The lower the permeability the larger the membrane area needed or the number of membrane modules for the given gas volume and time factor. Lower selectivity requires more steps in the separation with more complex operations, typically leading to higher costs. Large volume separations, such as O_2/N_2 for oxy-combustion or CO_2/CH_4 for natural gas treatments require highly permeable membranes. In some cases ultrahigh membrane selectivity is not necessarily desirable for large-scale gas separations, as for example, CO_2 separation from natural gas. This is because the permeate concentration of the more permeable gas reaches a plateau even as the selectivity continues to increase. Thus, a membrane with very high permeability and good selectivity may be more industrially attractive for large-scale applications.[12] In many industrial gas separations, process economics also limits the pressure ratio (feed pressure/permeate pressure) that can be used. As a consequence, the optimum membrane may not be the one with the highest selectivity, and membranes with different selectivities may be preferred in different portions of separation plants.[13] The factors that influence the process economics and thereby determine the properties of the optimum membrane are illustrated in Figure 1.

Highly permeable membranes are always the aim in the development of new materials, but the optimum membrane selectivity depends on the process and the operating conditions, especially the pressure ratio. The cost of the compressor package may be much more than the cost of the membrane unit, and the cost of electricity used to power the compressor is usually the largest operating expense. For these reasons, pressure ratios used in industrial processes are normally below 20, and are typically in the range of 5−15. The compressor/vacuum energy use is directly related to the membrane pressure ratio (Figure 1). A competitive process requires an affordably low pressure ratio, and this determines the preferred membrane selectivity.[13] Calculations of Merkel et al.[12] on the design for a postcombustion CO_2 capture process with membranes shows that at a given pressure ratio a trade-off exists between membrane area and permeate CO_2 concentration, which results in a narrow range of optimum selectivity for this separation. Even for a more selective membrane, the process would still require a larger membrane area to improve the purity of CO_2 in the permeate gas stream.

1.2. Membrane Material and Shape. In commercial biogas purification, feed streams typically contain a high fraction of CO_2 and impurities like H_2S and H_2O. Conventional biogas purification is achieved through CO_2 and H_2S gas absorption in suitable solvents, but absorption processes are highly energy-intensive and not well-suited for large-scale applications due to the large size and weight of the process equipment. Membranes used for industrial biogas purification are made from cellulose acetate and separate small polar molecules such as CO_2, moisture, and the remaining hydrogen sulfide.[14] Currently, the benefits of CO_2 removal by membrane plants, including low capital cost, high energy efficiency, and high product recovery, are restricted by challenges such as membrane plasticization, low contaminant resistance, and lower product purity than solvent absorption.[15] Plasticization is the phenomenon that the permeability of both components increases and the selectivity decreases. This is caused by an increase in the segmental motion of polymer chains at high feed pressures due to the presence of one or more sorbates.[16]

Another important constraint in the development of membrane applications is the inverse correlation between permeability and selectivity. Organic polymer membranes are particular susceptible to this gas permeability and selectivity relationship, such that membranes with high permeability have a low selectivity and vice versa. The well-known Robeson plots[17,18] for gas pairs, or related plots for pervaporation from Lue and Peng et al.,[19] summarize the permeability and selectivity of known dense membranes and thereby illustrate that as permeability increases the selectivity of the membrane decreases, giving an upper bound of membrane performance (Figure 2). These upper bounds of performance for organic

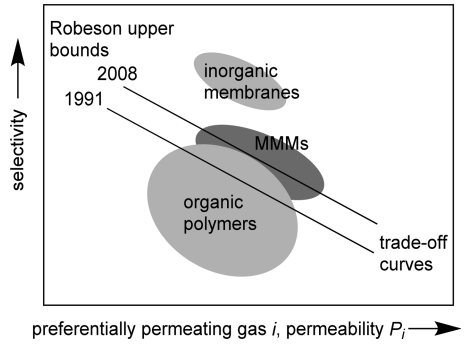

Figure 2. Schematic presentation of the inverse correlation (trade-off) between permeability and selectivity of dense membranes in gas separation with the 1991 and 2008 Robeson upper bounds.[17,18] Technologically interesting and better performing membranes lie around or above the Robeson upper bound. Figure reproduced from ref 28 with permission. Copyright Royal Society of Chemistry, 2012.

polymer membranes increase gradually with further development, but these do not approach the performances observed by other materials, for example, inorganic membranes. Efforts are being undertaken to pass this "Robeson upper bound" by the development of new polymeric materials,[20] pure inorganic membranes like zeolites (crystalline, porous aluminosilicates),[21,22] metal−organic frameworks (MOFs),[23] carbon molecular sieves (CMS),[24,25] carbon nanotubes (CNTs),[26] and graphene[27] or by combining different materials in so-called mixed-matrix membranes (MMMs) (see below).

Pure (also called *continuous*) inorganic zeolite or hybrid MOF membranes combine very good selectivity with high permeability.[29−32] The problems with fabricating such continuous membranes from individual microcrystals is the defect-free preparation and mechanical stability of the membrane during operation. The occurrence of cracks or holes will result in a loss of selectivity. There are numerous studies on sophisticated and specialized engineering techniques to produce supported MOF[33,34] and zeolite[31,35,36] thin films as a selective layer. Fabrication of a mechanically strong and stable, well-intergrown defect-free pure MOF membrane is still challenging and difficult to scale up for industrial application.[31,32,37,38]

DOI: 10.1021/acs.cgd.7b00595
Cryst. Growth Des. 2017, 17, 4467−4488

MMMs consist of a micro- or nanosized additive or filler component which is dispersed in the continuous organic polymer phase (Figure 3).[28,35,39−55] MMMs target the

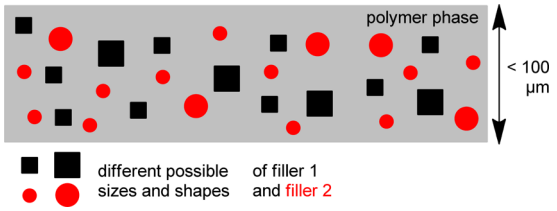

Figure 3. Schematic representation of a mixed-matrix membrane with two different additives (fillers), thereby also indicating different possible sizes, shapes, and components for the inorganic filler materials. Figure taken from ref 28 with permission. Copyright Royal Society of Chemistry, 2012.

combination of the good flexibility and processability of polymers and the very high gas separation performance of porous inorganic materials to thereby surpass the Robeson upper bound.[18] The addition of fillers to polymer materials can also meet the challenges of commercially used polymer materials, like membrane plasticization, low contaminant resistance, and low product purity and provide high performance gas separation MMMs, on the condition that defects at the filler−polymer interphase can be avoided. Various porous or nonporous inorganic additives have been tested as filler materials.[18,28,35,39,42−57] Improvements in membrane separation performance are expected for nanostructured porous additives such as zeolites or MOFs with size-selective adsorption and separation properties.[39,44] Concerning the filler, its chemical properties, functional groups on the surface, the distribution of particle sizes, and its shape are other important variables.

Gas separation MMMs are produced in different shapes: on the one hand symmetrical MMMs, in which the filler particles should be uniformly embedded in the polymer matrix, and on the other hand asymmetric MMMs, which consist of a thin polymer layer with filler and a thicker, porous carrier layer. Membranes used in industrial applications are usually integrated as asymmetric membranes which can be produced as flat sheets or as hollow fibers.[58]

Flat asymmetric MMMs can be prepared by the phase inversion method. The polymer and filler dispersion is poured onto a flat surface and solidifies after solvent exchange. During solidification, defects can occur within the membrane or on the surface. To minimize the defects on the surface an additional layer of polymer can be applied by spin coating.[59] The additional polymer layer can also be chemically cross-linked to the membrane layers which can increase the thermal and chemical stability as well as the selectivity usually with reduction in permeability.[60,61]

Asymmetric hollow fiber membranes are a focus when there is the problem of low gas flow through the membrane. Because of the high membrane area per module volume, the high packing density and the high gas flow through the hollow fiber, this membrane shape is optimal for industrial applications, as seen from an engineering and process economics point of view. In the preparation of MMM hollow fibers either a layer of the polymer−filler dispersion is applied onto the already prefabricated hollow fiber substrate, or the hollow fiber is directly fabricated from the target material.[62,63]

In the development of novel polymer and filler materials, and the investigation of effects of polymer and filler interaction, a symmetrical MMM is often chosen because the comparability of the production methods is better and effects on separations can be discussed more easily from a chemical point of view. The step toward module design and optimization of the membrane area/module volume is done in the engineering process. Such membrane shape and engineering aspects are significant for the industrial future of new membrane materials, including MMMs but go beyond the scope of this review.

1.3. Zeolites and MOF Additives−Background and Opportunities for MOFs. MOFs have been investigated as inorganic−organic hybrid additives for MMMs[64−69] as they are highly porous and should be able to interact better than purely inorganic zeolites with the surrounding polymer. MOFs have adaptable chemical properties and porosities through the metal−linker combination.[70] The interaction of the organic ligands of the MOF with the polymer, which can be enhanced with functional groups for specific supramolecular or even covalent bonding, should prevent interfacial microgaps, which lead to loss in selectivity.[28,35,42−44] In order to obtain materials with optimized separation properties, a perfect interaction between the two components is highly important for the preparation of MMMs.

Gas separation is the most studied field with MOF-MMMs, which is due to the very similar size of the substances in gas mixtures and microporous fillers with designable pore characteristics. The types of gas separations investigated with MOF-MMMs include CO_2/CH_4 separations for natural gas sweetening and biogas purification, CO_2/N_2 for the purification of flue gas streams, precombustion H_2/CO_2 capture, and air separation (O_2/N_2).[64]

Lab-scale adsorptive gas separation and purification processes have already shown the high potential of MOFs as a porous material compared to other adsorbers.[23,71] It has been reported that Mg and Fe-MOF-74, packed in a column, exhibit enhanced CO_2 separation from methane and C_1 to C_3 hydrocarbons.[72,73] Another example, where the overall capacity of the MOF material outperformed commercially available activated carbon materials as adsorbents, namely, Norit (type RB4) and CarboTech (type C38/4), is the removal of tetrahydrothiophene (THT) from natural gas in a fixed bed reactor.[74] The outstanding molecular size cutoff properties and high selectivity of MOFs would be maximally utilized in a neat supported layer prepared from intergrown MOF crystals. However, when MOFs are used as a filler in MMMs it is still possible to access their separation properties with high filler loading, but there will always be a compromise with the separation properties of the polymer-matrix, which is in most cases less efficient than the pure MOF material.

Zeolites possess a sharp molecular "cut-off" when used as fillers or neat, supported membranes, due to their fixed pore size and have been one of the most common inorganic materials used for the preparation of MMMs.[31,45] Because of their molecular sieving properties, they have been an extensively studied class of materials for membrane fabrication in multiple membrane forms and shapes (hollow fiber, supported molecular sieve membrane) with focus on industrial separation.[75,76,35,77] Zeolite membranes can exhibit remarkable separation properties, when they are fabricated as composite membranes which consist of a zeolite top layer on a mesoporous ceramic or metal support.[30] The company NGK INSULATORS, LTD has developed and produced a pure,

DOI: 10.1021/acs.cgd.7b00595
Cryst. Growth Des. 2017, 17, 4467−4488

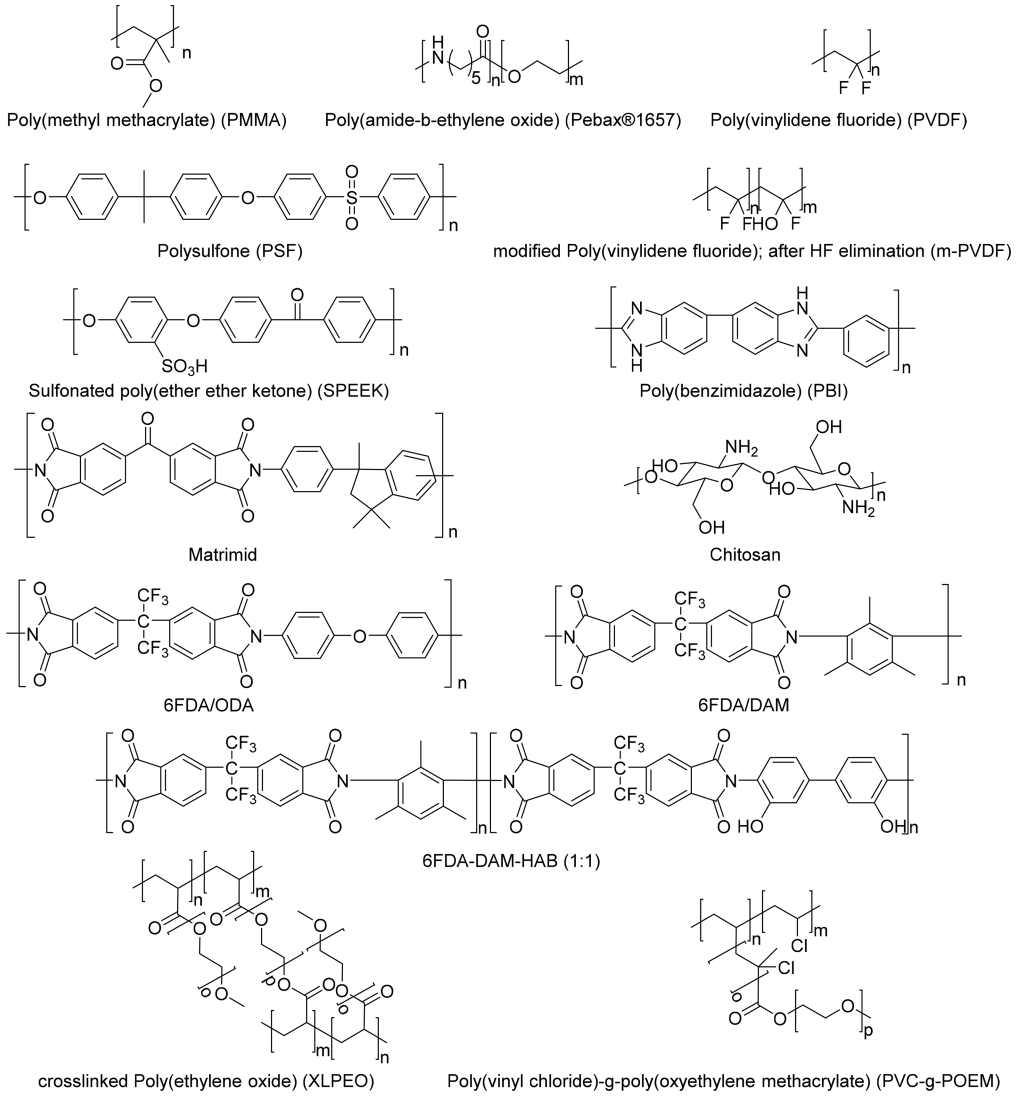

Figure 4. Repeat units of commercial polymers which are frequently used in polymer/MOF MMMs.

supported *MFI*-type (ZSM-5, *five*) zeolite gas separation membrane by forming a film on a porous ceramic substrate, which extracts *p*-xylene from xylene isomers produced in the petroleum refinery process. For the refinement of biogas generated from raw garbage by fermentation, a deca-dodecasil 3R (DDR)-type zeolite membrane was developed by the same company. This is also supported on a porous ceramic substrate and could isolate CO_2 from a mixture of methane and CO_2.[78] For neat, supported MOF-membranes, phenomena like "gate opening" and "breathing" make it hard to obtain the theoretical selectivities (cut off because of pore size) when MOFs are processed as a thin-film membrane.[31] Despite this, MOF/polymer MMMs usually show improved fluxes compared to pure polymer membranes and zeolite-based MMMs. Additionally, water is known to inhibit the CO_2 adsorption capacity of zeolites due to CO_2 and water competition for the sorbent sites.[79] These effects are also known for MOFs, but in certain instances, such as the case of hydrated MIL-101, terminal water molecules can act as additional binding sites for CO_2 adsorption, promoting CO_2/CH_4 separation at low pressures.[80] These reasons make MOFs a preferred material, when processed as fillers in polymer/MOF MMMs, while zeolites are superior, when processed as supported thin-film membranes.[31]

Besides gas separation, industrially interesting separation technologies include liquid filtration like nanofiltration and pervaporation. The field of MOF-MMMs has also expanded to these applications and has been the subject of recent reviews.[81,82] For example, in organic solvent nanofiltration from styrene oligomers, the addition of MIL-101(Cr) to a polyamide (PA) matrix showed a remarkably increased flux while preserving rejection.[83] Further, the combination of MIL-101(Cr) and ZIF-11 in a polyamide thin film nanocomposite membrane resulted in an enhanced and versatile membrane for organic solvent nanofiltration from organic dyes combining the high porosity of MIL-101(Cr) and the hydrophobicity of the ZIF-11.[84] In pervaporation the separation of water from ethanol was carried out with a HKUST-1/Matrimid MMM, at 40 wt % the addition of HKUST-1 to the MMM led to an increased flux of 0.43 kg m^{-2} h^{-1} (compared to 0.24 kg m^{-2} h^{-1} for pure Matrimid) without decreasing selectivity due to the hydrophilicity of HKUST-1.[85]

1.4. Challenges with MOF Additives. The hydrothermal stability of the MMM, including the filler material, is a crucial issue. It is not economically possible to fully dry industrial gases

DOI: 10.1021/acs.cgd.7b00595
Cryst. Growth Des. 2017, 17, 4467−4488

before separation to prevent membrane degradation. On the contrary, the membrane and its components must be stable toward moisture. Unfortunately MOFs, which are metal−ligand coordination compounds, are inherently unstable toward reaction with water and linker displacement by aqua ligands.[86,87] Zinc-carboxylate MOFs, such as MOF-5 and the IRMOF-series, have a low moisture stability, whereas HKUST-1 ($Cu_3(BTC)_2$) is intermediate but eventually decomposes.[86,88−90] MIL-type compounds, including MIL-101(Cr),[91−93] NH_2-MIL-53(Al), Al-fumarate,[89,94] CAU-10-H[95] and ZIF-8, exhibit higher water stability.[86,88−90,96,97] Therefore, hydrolytically stable MOF materials must be employed as additives for MMMs to have a realistic chance for further technical development. Concerning other contaminants in biogas purification, and in pre- and postcombustion CO_2 separation, gases such as H_2S, SO_x, NO_x, CO, NH_3 are known as membrane poisons, effecting the separation process by plasticization and aging effects or degradation of the material. Testing MOFs for not only water stability, but also pH dependent stability, shows that the chemical stability toward acids and bases is overall disappointing, but again MIL-101(Cr), MIL-53(Al), and UiO-66(Zr) gave the best results concerning pH stability.[87] MOFs are studied for the adsorptive removal of hazardous compounds from gas streams and air, and their adsorptive capacities have shown excellent potential. However, there is a lack of studies which discuss their regenerability, i.e., stability.[98] Many of pristine MOFs are often not suitable for the sorptive treatment of highly reactive and corrosive gases such as H_2S and SO_2. To overcome this limitation structural functionalization of MOFs can be utilized.[99]

1.5. Scope of this Review. MOFs are widely studied as fillers in mixed matrix membranes and compared for their impact on the separation performance of pure polymer materials.[28,31,38,64] Most reported studies on the preparation and characterization of MOF-based MMMs are often fundamental, but herein we present an analysis of these results to develop an understanding of the separation mechanisms, the role of the MOFs and the effect of the polymer/MOF particle interface. This knowledge is needed to develop MOF-MMMs which are suitable for industrial applications. MOF-MMMs have been the subject of recent reviews.[28,32,37,44,64] In this review, the current trends of MMM fabrication will be examined with a focus on recent significant developments in the MMM field concerning MOF and polymer compositions and newer aspects, such as the role of particle size and shape control in MOF-MMM fabrication. This will demonstrate how developments in membrane separation performance can be advanced through the incorporation of designed MOF additives. With MOF-MMM works expanding to higher complexity and more material combinations, the new synthetic approaches for MOF additives need updating in a comparative manner to point out the successful strategies which could lead to the fabrication of high performing MMMs. The impact of these additives on the separation performance is analyzed by the comparison of the permeability and selectivity data of the highlighted MMMs and corresponding polymer membranes. The numerical values are summarized in Table 1. To provide guidance on the shape and structural dimension of pore sizes and secondary building units of the frameworks, images and structure descriptions of the MOF-fillers are given in the Supporting Information. The membrane polymers, which are noted in the following sections, are depicted in Figure 4 with their repeat unit.

2. SIGNIFICANT DEVELOPMENTS OF MOF INCLUSION IN MMMS

2.1. Linkers with Functional Groups. MOFs with polar functional groups on their linkers can give a better selectivity for one of the gases in a mixture.[100] Polar functional groups such as amine, $-NH_2$, hydroxo, $-OH$, nitro, $-NO_2$, and sulfonic acid $-SO_3H$ on the linkers in MOFs like NH_2-MIL-125(Ti)[101,102] or HSO_3-MIL-101(Cr)[103] improve interactions with CO_2 due to their polarizability and/or hydrogen bonding interactions with the CO_2 molecule.[104] Further, the suitable selection of a corresponding polymer can enhance the polymer/MOF-particle interface interaction. Especially in polyimides, interactions such as hydrogen bonding between the polymer backbone and the surface-functional groups of the MOF filler particle led to increased compatibility. The improved gas separation properties of MMMs based on amine-containing MOFs, including NH_2-UiO-66(Zr) and NH_2-MOF-199 (MOF-199 is also known as Cu-BTC or HKUST-1),[41] NH_2-MIL-53(Al),[40,55,105,106] and NH_2-MIL-101(Al),[105,106] were explained accordingly.

A good comparison is provided by a polysulfone (PSF)/NH_2-MIL-125(Ti)[101,102] MMM where the selectivity for CO_2/CH_4 separation dropped at high filler loadings (30 wt %) because of voids from poor polymer−filler adhesion.[107] On the other hand, a Matrimid/NH_2-MIL-125(Ti) MMM at 30 wt % loading showed a 550% increase in CO_2/CH_4 selectivity together with 35% higher CO_2 permeability than the PSF MMM (Figure 5).[108] We note, however, that no spectroscopic proof was given for the anticipated hydrogen or even covalent bonding between the polyimide and NH_2-groups on the MOF surface.[109]

HSO_3-MIL-101(Cr)[103] MMMs[110] exhibited a better CO_2/CH_4 gas selectivity (50 at a CO_2 permeability of 2064 Barrer) compared with the MMM from unmodified MIL-101(Cr) (31 at a CO_2 permeability of 1600 Barrer). In both of these MMMs humidification or bound water led to increased CO_2

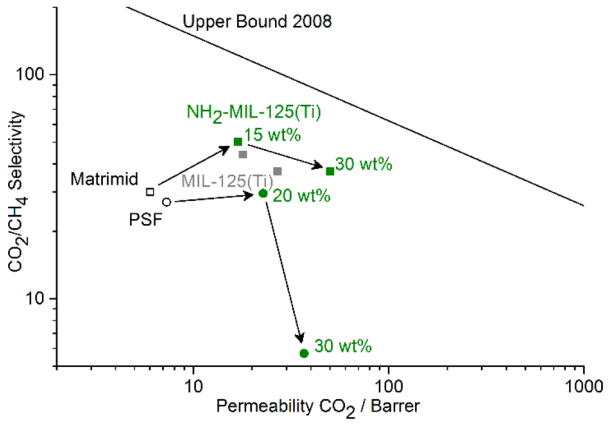

Figure 5. Comparative CO_2/CH_4 permselectivity and upper bound plot for Matrimid/MIL-125(Ti) MMMs (squares) with unmodified MIL-125(Ti) (gray) and NH_2-MIL-125(Ti) (green) for different MOF/MMM mass fractions[108] and PSF-based MMMs (circles) with NH_2-MIL-125(Ti) with a strong drop in selectivity at higher filler loading.[107] See Supporting Information for a graphic and structure description of MIL-125.[101]

DOI: 10.1021/acs.cgd.7b00595
Cryst. Growth Des. 2017, 17, 4467−4488

permeability and improved selectivity (Figure 6). Hydrated sulfonic acid groups will improve hydrophilic CO_2 solubility in

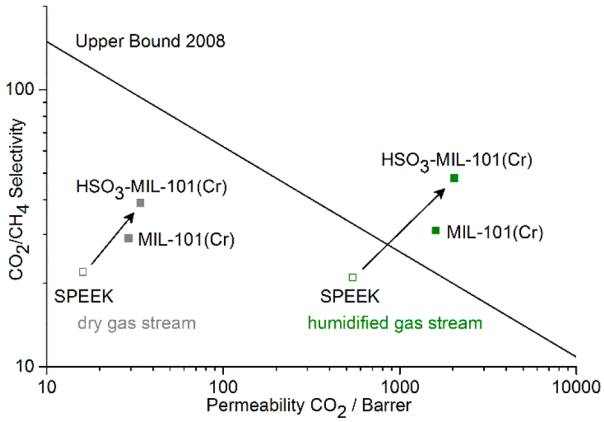

Figure 6. Comparative CO_2/CH_4 permselectivity and upper bound plot for sulfonated poly(ether ether ketone) (SPEEK)/MIL-101(Cr) MMMs with 40 wt % nonfunctionalized or sulfonated MIL-101(Cr). Permeability and selectivity show a strong increase, when a humidified gas stream (green) is used, compared to dry gas streams (gray).[111] See Supporting Information for a graphic and structure description of MIL-101.[91]

the MMM and thereby lead to increased permeability and selectivity over hydrophobic CH_4.[111] The sulfonic acid groups from both the polymer matrix, which was a sulfonated poly(ether ether ketone) (SPEEK), and the sulfonated MOF may construct facilitated transport pathways for CO_2 and, thereby, improve CO_2 solubility and selectivity (cf. Figure 13). We note that the SPEEK polymer itself, with sulfonic acid as hydrophilic groups, can adsorb up to 11 wt % water with a sulfonation degree of 67%.[112,113] As a hydrogel with $-SO_3H$ groups, humidified SPEEK already has a relatively high CO_2 selective solubility which is beneficial for CO_2 transport based on the solution-diffusion mechanism.[113]

2.2. Modulated MOF-Synthesis. Linker or node modification of known MOFs can be used to improve the MOF–polymer interaction and thereby the separation performance of the MOF-MMM (see above).[38,45] Such linker modification can be carried out by replacing the linker in the initial MOF-synthesis, or by so-called postsynthetic linker modification (PSM)[114−117] and solvent-assisted linker exchange (SALE).[118,119] Postsynthetic modification (PSM) of MOFs refers to the alteration of a MOF framework after its synthesis, for example, through chemical reaction of the linker (covalent PSM), solvent ligand replacement on the metal (grafting, dative PSM) or postsynthetic deprotection of a functional group on the linker (PSD) (Figure 7).[116,120−122] The technique permits functionalization of the MOF crystallites while retaining the overall framework structure and porosity.[123]

Besides the MOF linker and node, also the MOF crystal size, particle morphology, and outer surface ligands can be adjusted. This is, for example, done by using monodentate carboxylate ligands, monatomic anions or surfactants as so-called "modulators" during the synthesis of the MOF. The modulators compete with the actual linkers for coordination to the metal sites. Modulators may lead to particles of similar and desired size, as well as particles possessing a specific surface chemistry due to capping with modulator molecules.[124−126]

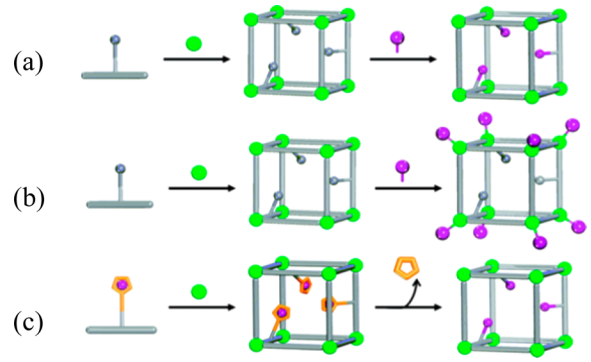

Figure 7. Schematic depiction of synthetic approaches to modify a MOF after synthesis. The different routes are specified after the type of chemical bond that is formed or broken during the postsynthetic approach for (a) chemical reaction on the linker (covalent PSM), (b) ligand replacement on the metal (dative PSM), and (c) postsynthetic functional group deprotection (PSD). Figure reproduced with permission of the American Chemical Society. Reprinted with permission from ref 122. Copyright 2012 American Chemical Society.

Benzoic acid (BA) and 4-aminobenzoic acid (ABA) were added as modulators in the synthesis of UiO-66(Zr)[127,128] and NH_2-UiO-66(Zr)[124] in a 50:1 molar ratio relative to the linker. Reaction of the amine groups on the MOF surface was seen by the appearance of amide signals in the IR spectra of Matrimid MMMs with high amino-MOF filler loading. The membrane of Matrimid/NH_2-UiO-66(Zr)-ABA gave the best performance in CO_2/CH_4 mixed-gas separations being over 50% more selective and 540% more permeable than the continuous Matrimid membrane and 30% and 140% more selective and permeable than the Matrimid/UiO-66(Zr) MMM (Figure 8).[129]

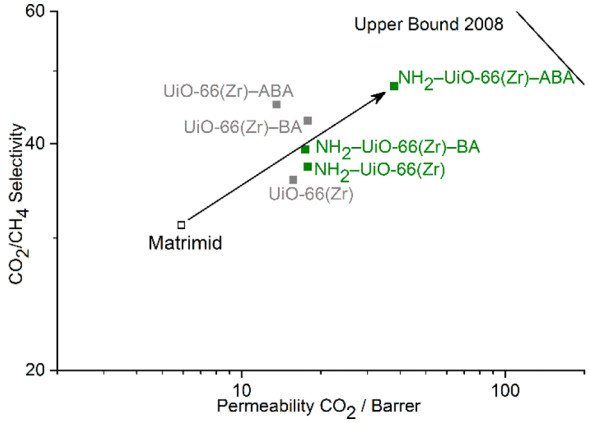

Figure 8. Comparative CO_2/CH_4 permselectivity and upper bound plot for Matrimid/UiO-66(Zr) MMMs with 30 wt % standard UiO-66(Zr) (gray) and amino-functionalized NH_2-UiO-66(Zr) (green) in addition with benzoic acid (BA) or aminobenzoic acid (ABA) used as modulator during the UiO-66(Zr) synthesis.[129] See Supporting Information for a graphic and structure description of UiO-66.[127,130]

Another aspect with high impact on the separation properties of the MMM material, besides the above-mentioned chemical functionality of the linker, is the pore size and shape of the MOF-filler. The pore aperture (pore window diameter) in ZIF-8[131,132] is about 3.4 Å, so it could be assumed that a ZIF-8 membrane should be able to separate CO_2 with a kinetic diameter of 3.3 Å from larger gas molecules such as CH_4 with a kinetic diameter of 3.8 Å. However, this cutoff size cannot be

DOI: 10.1021/acs.cgd.7b00595
Cryst. Growth Des. 2017, 17, 4467−4488

observed in gas permeation measurements. Neat ZIF-8[132] membranes exhibit only moderate CO_2 selectivities, and CH_4 can slowly pass through the ZIF-8 pore network, resulting in no sharp cutoff at 3.4 Å.[133,134] This is rationalized to be due to the flexibility of the ZIF-8 network.[135] A reduction of the cutoff size of ZIF-8 for CO_2 separation was achieved by incorporating room-temperature ionic liquids (RTILs) into the ZIF-8 cavities through an ionothermal synthesis of ZIF-8 in the RTIL butyl-methyl imidazolium bis(trifluoromethyl-sulfonyl) imide, [bmim][Tf_2N], which also shows good affinity to CO_2. The pore size distribution calculated from N_2 adsorption measurements indicated that the effective cage size of ZIF-8 was remarkably reduced after incorporation of the IL.[136] For a 6 wt % PSF/IL@ZIF-8 MMM the selectivities of CO_2/N_2, and CO_2/CH_4 were remarkably improved from 29 to 115 and from 19 to 34 at only slightly reduced CO_2 permeability compared to MMMs with unmodified ZIF-8 (Figure 9). The affinity of the IL for CO_2 dissolution[137] may have helped in the increase in selectivity.

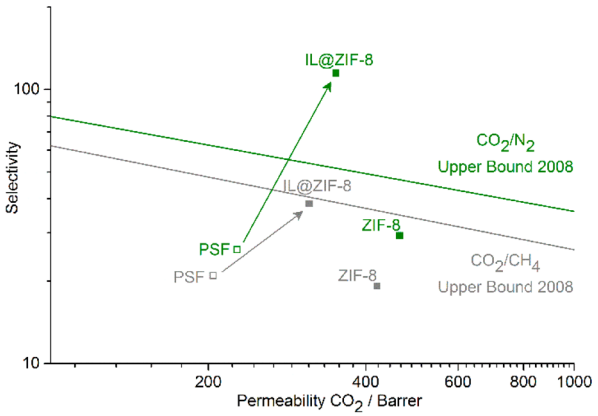

Figure 9. Permeability and selectivity of PSF/IL@ZIF-8 MMMs compared to ZIF-8 MMMs and the pure polysulfone (PSF) membrane. CO_2/CH_4 (gray) CO_2/N_2 (green) permselectivity; the mixed gas permeabilities were measured at 30 °C and 6 bar pressure difference. Membranes were prepared by dip coating of the polymer or polymer/MOF mixture on an asymmetric gamma aluminum disc. This preparation method results in significantly higher permeation rates than for neat self-supported polymer films.[136] See Supporting Information for a graphic and structure description of ZIF-8.[131,132]

A thin polydopamine (PDA) coating (from polymerization of dopamine hydrochloride) was applied on the particles of the MOF NH_2-CAU-1[138] as a solubilizer for the poly(methyl methacrylate) (PMMA) matrix.[139] The PMMA/NH_2-CAU-1@PDA MMM showed a high O_2 and low CO_2 permeability with increased ideal O_2/CO_2 and O_2/N_2 selectivity over an MMM formed with noncoated NH_2-CAU-1 (Figure 10).[139] Pure PMMA films were not fabricated or characterized in this work, which is often necessary to prove the accuracy of the characterization methods. Thereby the permselectivities of the MMMs are multiple orders of magnitude higher than the rare values found in the literature for pure PMMA.[140,141]

NH_2-UiO-66(Zr) was postsynthetically modified with polar succinic acid (HO_2C-$(CHOH)_2$-CO_2H), nonpolar decanoyl chloride (n-$C_9H_{17}COCl$), or aromatic phenyl acetyl chloride (PhCOCl) (covalent PSM with amide bond formation) and combined with Matrimid to give MMMs for CO_2/N_2 single gas permeation measurements.[123] Larger PhCOCl and n-$C_9H_{17}COCl$ molecules cannot diffuse into the MOF pores

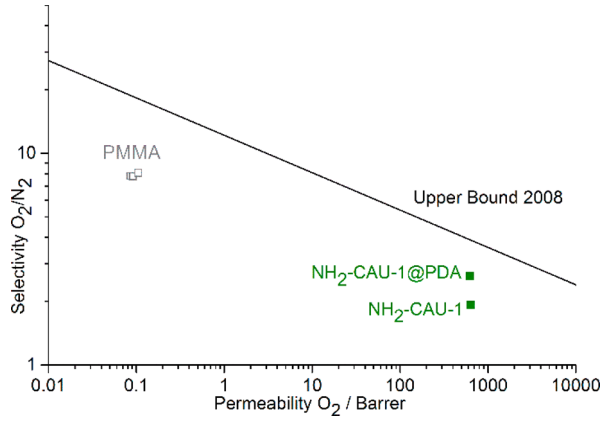

Figure 10. O_2/N_2 permselectivity and upper bound plot for PMMA/NH_2-CAU-1 MMMs (green) with and without polydopamine (PDA) coating.[139] The very rare literature values for pure PMMA membranes[140,141] (gray) were added for comparison to the permselectivity of the MMMs and are not necessarily correlated with the reported MMM values. See Supporting Information for a graphic and structure description of CAU-1.[138]

and react only with the amine groups on the MOF particle surface. The smaller succinic acid reacted also with the internal amino groups. The imide groups in the Matrimid polymer can interact with the MOF-NH_2 groups or PSM−amide linkages through hydrogen bonding (Figure 11). Aromatic rings from

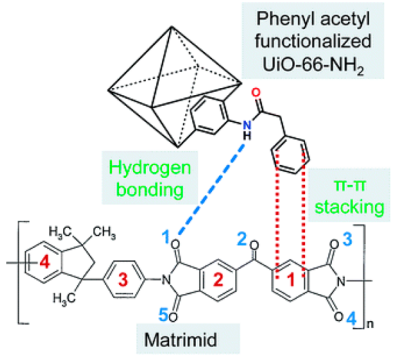

Figure 11. Possible interactions between the Matrimid polymer and phenyl acetyl functionalized NH_2-UiO-66(Zr). Figure reproduced from ref 123 with permission. Copyright Royal Society of Chemistry, 2015.

PhCO- can further interact through $\pi-\pi$ stacking. While no spectroscopic evidence for such polymer−MOF interaction was provided, Matrimid and PSM-NH_2-UiO-66(Zr) showed good film formation, and no cavity formation around the particles was seen by scanning electron microscopy (SEM). MMMs with the aromatic PhCOCl-functionalized NH_2-UiO-66(Zr) showed an increase in CO_2/N_2 selectivity and CO_2 permeability over unmodified NH_2-UiO-66(Zr), while the polar and nonpolar modification gave a decrease in selectivity (Figure 12).

Employing dative PSM, polyethylenimine (PEI) of low molecular weight (300 Da) was immobilized on and in MIL-101(Cr)[91,142] possibly by grafting to the metal sites (dative PSM, cf. Figure 7b), although spectroscopic proof for the coordination of the amine group onto the metal sites in MIL-101(Cr) was lacking.[143−146] IR spectroscopy on the MMM formed from SPEEK/PEI@MIL-101(Cr) indicated hydrogen bonding between SPEEK sulfonic acid groups and PEI amine

DOI: 10.1021/acs.cgd.7b00595
Cryst. Growth Des. 2017, 17, 4467−4488

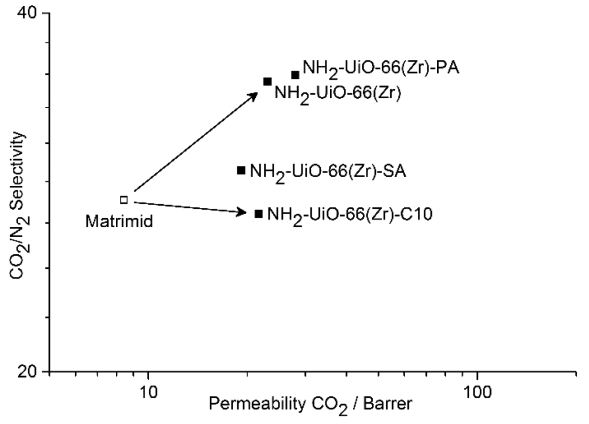

Figure 12. Comparative CO_2/N_2 permselectivity for Matrimid MMMs with NH_2-UiO-66(Zr) postsynthetically functionalized with succinic acid (SA, HO_2C-$(CHOH)_2$-CO_2H), decanoyl chloride (C10, *n*-$C_9H_{17}COCl$) or phenyl acetyl chloride (PA, PhCOCl).[123] See Supporting Information for a graphic and structure description of UiO-66.[127,130]

groups presumably at the polymer−MOF interface. SPEEK itself is known to change its perm-selectivity when water is absorbed because of the hydrophilic sulfonic acid groups leading to formation of a hydrogel. This is connected to high CO_2 selective absorption which is in turn beneficial for CO_2 transport based on the solution-diffusion mechanism.[112,113] CO_2 can react with the abundant PEI amine groups in the humidified SPEEK/PEI@MIL-101(Cr) membrane producing, via the carbamate, alkyl ammonium groups, and HCO_3^- (Scheme 1), which could then facilitate CO_2 transport by "HCO_3^- ion hopping" from one ammonium site to another (Figure 13).[113]

Scheme 1. Reaction Scheme for the Reversible Chemical Absorption of CO_2 by Primary Amines to Carbamate and in the Presence of Water to Hydrogen Carbonate Products

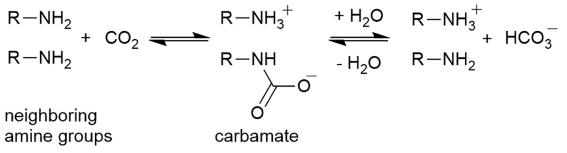

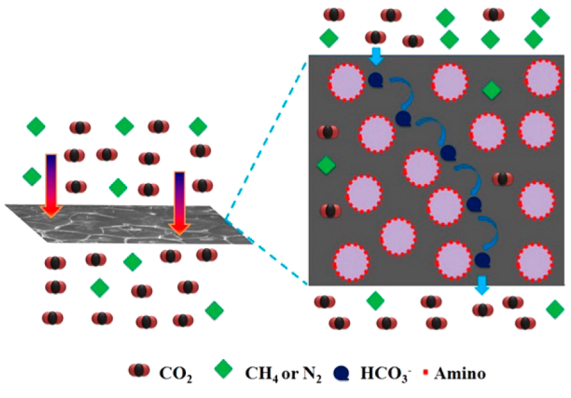

Figure 13. Facilitated transport pathway of CO_2 in amino-containing MMMs where the reversible reaction between facilitated transport carriers and CO_2 molecules enhances the CO_2 separation performance. Figure reproduced from ref 113 with permission. Copyright Elsevier 2014.

Gas permeation experiments showed that the PEI@MIL-101(Cr) filled MMMs outperformed those prepared from unmodified MIL-101(Cr) and pure SPEEK. The CO_2 permeability, CO_2/CH_4 selectivity, and CO_2/N_2 selectivity all increased with the PEI@MIL-101(Cr) filler content. The membrane loaded with 40 wt % PEI@MIL-101(Cr) exhibited the highest selectivity of 72 and 80 for CO_2/CH_4 and CO_2/N_2 mixtures, respectively, with a CO_2 permeability of 2490 Barrer at 1.0 bar and 25 °C (Figure 14). Further, there was a strong

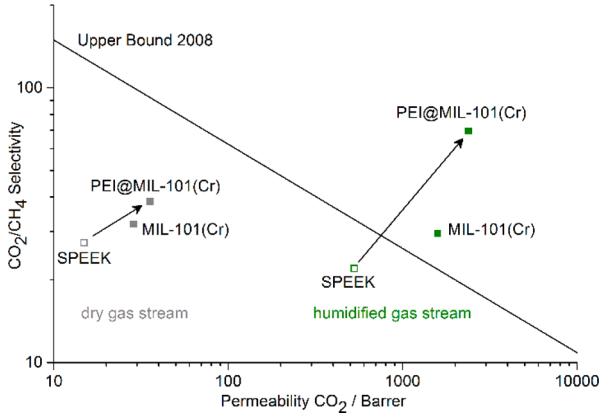

Figure 14. Comparative CO_2/CH_4 permselectivity and upper bound plot for sulfonated poly(ether ether ketone) (SPEEK)/MIL-101(Cr) MMMs with 40 wt % nonfunctionalized MIL-101 or functionalized PEI@MIL-101. Permeability and selectivity show a strong increase, when a humidified gas stream (green) is used, compared to dry gas streams (gray).[143] Compare also to the case depicted in Figure 6 above. See Supporting Information for a graphic and structure description of MIL-101.[91]

correlation between total water content and the selectivity for CO_2/CH_4 and CO_2/N_2 gas selectivity. For water and CO_2 loaded membranes a sharp IR band at 2346 cm^{-1} was attributed to carbamate formation $RHNCOO^-$, and bands at 839 and 963 cm^{-1} were assigned to the subsequently formed HCO_3^- (Scheme 1) which could permeate through the MMM with lower energy barrier by the hopping mechanism (cf. Figure 13 above).[143]

The postsynthetic modification of MOFs requires the accessibility of the pores; otherwise reactants cannot diffuse into the channels and only react on the surface of the particles or at the pore openings. In many studies of MMMs the accessibility of the filler MOF pores are not the focus; typically the mechanical and morphological properties of the membranes and properties related to a specific separation are examined. Also the MOF loading is often relatively low (up to 30 wt %). For the specific characterization and understanding of a processable mixed-MMM material, the properties of the MOFs as an important component in separation processes should not be overlooked. Properties like pore shape, pore size, surface area, and chemical accessibility have an important influence on the transport mechanisms inside a MMM material and should be closely studied in relation to the transport phenomena. Cohen et al. have developed a technique to fabricate MMMs with very high MOF loading such that the properties of the composite material are not dominated by the polymer.[114] In these examples the loading is high enough (50−67 wt %) such that the composite material can no longer be viewed as a MOF filler in a polymer matrix but as MOF particles connected by a polymeric binder. This allows the

DOI: 10.1021/acs.cgd.7b00595
Cryst. Growth Des. 2017, 17, 4467−4488

MOF particles to dominate the properties of the membrane material, giving behavior approaching that of a pure MOF film but with better mechanical characteristics. Because of the limited particle and pore accessibility of MOF fillers in MMMs, the PSM of the fillers is usually carried out before incorporation into the polymer matrix.[38,45] Here, in this case, PSM was possible in the membrane material, demonstrating that the MOF filler was functionally accessible. For this purpose, a UiO-66 MMM was immersed in a solution of NH_2-bdc for 24 h at 55 °C which resulted in a postsynthetic exchange (PSE) reaction to give UiO-66-NH_2 MMMs, with approximately 33% of the bdc ligands exchanged for NH_2-bdc.

The technique can be used for inclusion of a diverse range of MOFs into the polymer poly(vinylidene fluoride) (PVDF). The MOFs used in Cohen's studies were of UiO-66,[130] HKUST-1,[147] MIL-101,[91,148] MIL-53,[149,150] and ZIF-8.[132] Conventional membrane preparation methods are carried out by solution casting (casting of a polymer solution with dispersed MOF particles) or by using a priming protocol (priming is a technique where the MOF particle suspension is combined stepwise with part of the polymer solution and sonicated to form a suspension, which avoids potential agglomeration of the filler material and reduces the stress at the particle−polymer interface). In contrast to this, for the preparation of MOF/PVDF MMMs, a mixture of solvents was used to prepare the polymer/MOF casting suspension. The MOF was first dispersed in acetone, a solvent with low viscosity and low boiling point; i.e., the dispersion of the particles is easy to achieve, and the solvent can be removed before casting. Then the polymer solution (7.5 wt % of PVDF in DMF or NMP) was added, followed by sonication again (to ensure the homogeneity of the mixed solvent system) and removal of acetone, to leave the dispersed particles in the viscous polymer solution.[114] The advantages of casting a viscous polymer solution with homogeneously dispersed fillers is that the film can be casted mechanically (with a blade) on a support and the particles are restricted in their movement during film formation, avoiding agglomeration, phase separation, or sedimentation. DMF or NMP can be removed at elevated temperature, resulting in flexible, mechanically stable membranes with the highest filler loading achieved for applicable MOF-MMMs.[64−69]

To test the applicability of these PVDF based MMMs, the PVDF/UiO-66 membranes were used for liquid filtration of Coomassie blue from an aqueous solution of methyl orange.[114] The HKUST-1 membranes were investigated for the selective uptake of ammonia from air. For the separation of ammonia from air, the water stability of HKUST-1 was tested under realistic conditions, including the presence of humidity in the gas mixtures.[151] HKUST-1 powder is not stable when exposed to water as confirmed by powder X-ray diffraction (PXRD) measurements, FTIR spectra and nitrogen adsorption (exposed to several different temperatures and relative humidity levels (% RH)). The most aggressive aging condition was 40 °C and 90% RH where the change of the HKUST-1 structure starts after 7 days, and changes in the IR spectra occur with the gradual appearance of bands at 1708 and 1243 cm^{-1} corresponding to the C═O and C−OH bands of a carboxylic acid. Also a decrease in the intensity of bands at 1650 and the 1422 cm^{-1} indicate the transformation of the HKUST-1 carboxylate nodes to their protonated acid analogues.[152] The PVDF/HKUST-1 MMMs were aged under the same conditions, and PXRD patterns remained unchanged over 28 days. Furthermore, FTIR spectra did not reveal the formation of the carboxylic acid bands. The bulk powder of HKUST-1 loses 90% of its capacity for ammonia uptake after 7 days aging, whereas for the MMMs only a change below 20% was observed. The MOF performance characteristics were retained in the MMMs utilizing PVDF as a binder, but the stability of the MOF material was increased significantly.

2.3. Polymer−MOF Hybrids (polyMOFs). Polymer−MOF hybrids (polyMOFs) have organic polymers built into MOFs or are MOFs constructed from organic polymer linkers. In one material these combine the advantages of flexible and easy to process polymer materials with the porosity of MOFs.[153,154] Consequently, the polymer−MOF hybrid materials are intended as neat membrane materials.

Structures of polyMOFs with the same topology (isoreticular) as MOF-5[155,156] and the IRMOF-*n* series,[157] as well as high porosity, can be synthesized from 2,5-substituted derivatives of H_2bdc or 2,2′-linked di-H_2bdc ligands[147,148] or 2,5-connected poly-H_2bdc ligands[153,158,159] (Figure 15). See

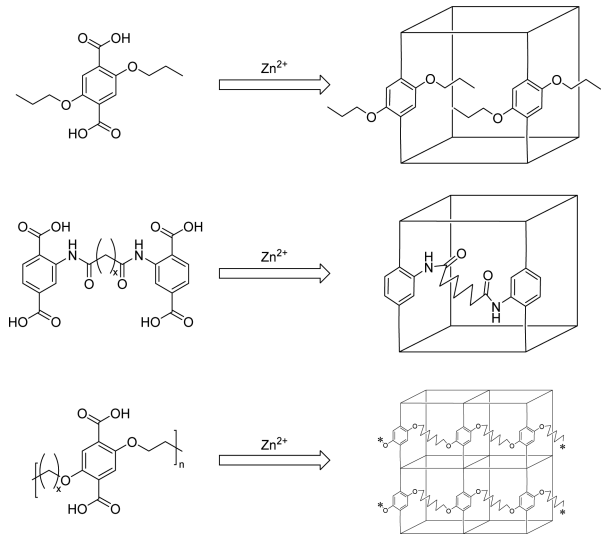

Figure 15. IRMOF derivatives constructed from (top to bottom): a H_2bdc ligand derivative, a 2,2′-linked di-H_2bdc ligand, and a polymeric H_2bdc polymer ligand with variable spacer length (x).

Supporting Information for a graphic and structure description of MOF-5.[155] A systematic investigation of the synthesis conditions of Zn-based poly MOFs with different spacer length showed that, depending on the temperature and spacer length of the 2,5-connected poly-H_2bdc, the resulting material morphologies ranged from spherical superstructures to crystalline films.[153]

Very high surface areas (S_{Lang} = 4000 m^2/g)[155,156] and selective adsorption of CO_2 over CH_4[160] make MOF-5 and other IRMOFs interesting as fillers in MMMs for gas separation.[161] However, Zn-carboxylate MOFs have the problem of rapid Zn-carboxylate hydrolysis when exposed to air humidity.[86,87] Contact angle measurements for the polyMOFs showed increased hydrophobicity of the material with a better stability against air/humidity, which should make separation tests as membranes more realistic. The polyMOFs have much smaller BET surface areas than MOF-5 because of the incorporation of polymer chains in the framework but adsorb more CO_2 due to stronger interactions in smaller pores.[162]

DOI: 10.1021/acs.cgd.7b00595
Cryst. Growth Des. 2017, 17, 4467−4488

A polyMOF could also be formed from Zn^{2+}, 4,4′-bipyridine (bpy), and a 2,5-connected poly-H_2bdc ligand, akin to the known mixed-ligand MOF $[Zn_2(bme\text{-}bdc)_2(bpy)]_n$ (bme-bdc = 2,5-bis(2-methoxyethoxy)-1,4-benzenedicarboxylate) (Figure 16).[163−165] The polyMOF formed particles which pack into

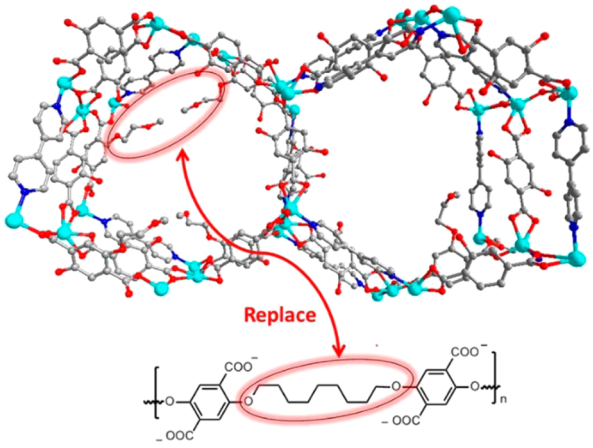

Figure 16. Structural representation of $[Zn_2(bme\text{-}bdc)_2(bpy)]]_n$ and design concept for polyMOF $[Zn_2(2,5\text{-}poly\text{-}bdc)_2(bpy)]_n$ by formal replacement of bme-bdc (2,5-bis(2-methoxyethoxy)-1,4-benzenedicarboxylate) with the 2,5-poly bdc ligand (bottom). This is an unofficial adaptation from ref 154 that appeared in an ACS publication. ACS has not endorsed the content of this adaptation or the context of its use.

uniform dense and defect-free films without any extra binder or polymer. These films exhibited relatively high CO_2 sorption but very low N_2 sorption, making them promising materials for CO_2/N_2 separation. The mixed-ligand polyMOFs also demonstrated good water or water vapor stability in contrast to the parent material $[Zn_2(bme\text{-}bdc)_2(bpy)]_n$.[154]

2.4. Functionalized Polymers for MMMs. Thus far in the review modifications of the MOF-fillers were presented without attention to changes in the polymers for the MMMs. As noted above, however, interesting behavior of MIL-53[149,166,167] composites with different polyimides has been observed when the structure of the polymer is altered by substitution of the diamine monomer to enhance the flexibility of the polymer chain.[105] MIL-53(Al)[53,55,168] and NH_2-MIL-53-(Al)[40,52,105,106,169] are two intensively examined fillers in MOF-based MMMs because they show good adhesion with different polymers and often act as a model system for the influence of the NH_2 group on the polymer filler interaction. Here the interaction of different polymers with (NH_2-)MIL-53(Al) is examined with a focus on polymer functionalization.

Basic polymer structures can be modified by covalent attachment of groups onto the polymer chain (grafting)[170] or by substitution of monomer units to introduce other functionalities. The influence of different diamine monomers in 6-FDA-based polyimides was investigated by studying the morphology and separation performance of NH_2-MIL-53 MMMs.[171] With 6FDA-ODA (6FDA = 4,4′-hexafluoroisopropylidene diphthalic anhydride, ODA = 4,4′-oxidianiline, cf. Figure 4), the MMMs showed a very low CO_2 permeability of less than 15 Barrer (Figure 17), together with MOF particle agglomeration and weak polymer−MOF adhesion.[53] Also in the 6FDA-DAM/NH_2-MIL-53 membrane (DAM = 2,4-diaminomesitylene) the MOF particles agglomerated into clusters separated from the polymer.[171] In contrast to these

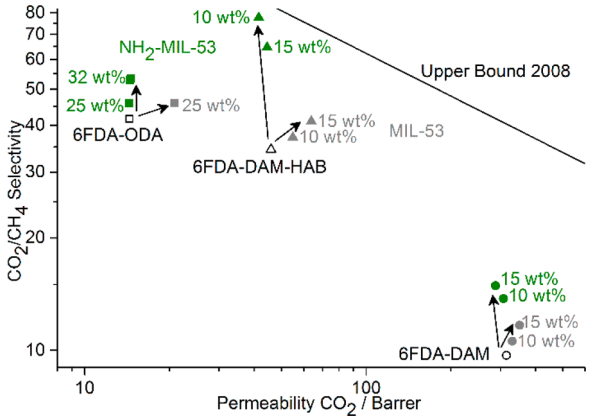

Figure 17. CO_2/CH_4 permselectivity and upper bound plot for 6-FDA based polyimides with different diamine monomers (ODA, DAM, and HAB) and their (NH_2-)MIL-53 MMMs with standard (gray) and NH_2-MIL-53 (green) for different MOF/MMM mass fractions. The influence of the fillers on permeability and selectivity are compared for 6FDA-ODA[53] (squares), 6FDA-DAM-HAB (triangles), and 6FDA-DAM[171] (circles). See Supporting Information for a graphic and structure description of MIL-53.[149,166,167]

6FDA-ODA and 6FDA-DAM based MMMs, membranes prepared from the copolyimide 6FDA-DAM-HAB (1:1) (HAB = 3,3′-dihydroxy-4,4′-diamino-biphenyl) and 10 wt % NH_2-MIL-53 approached the permeability/selectivity of the 2008 Robeson's upper bound (Figure 17). The hydroxyl groups in the HAB moiety were seen as the cause of a better interaction between the NH_2-MOF particles and the polymer matrix, giving an improved particle dispersion with no interfacial voids.[171]

These copolyimides, which have intrinsic permeabilities of 40−60 Barrer display relatively low permeabilities and high separation factors compared to other polyimides. The polymer poly(vinylidene fluoride) (PVDF), which acts more like a gas barrier with a CO_2 permeability of below 1 Barrer, was also studied. With a permeability this low, and a CO_2/CH_4 separation factor of 20 the influences of the filler on the separation process can be examined much more closely because the difference in flux and selectivity between polymer and filler is higher compared to most other studies. Thus, PVDF was studied as a model polymer even though it has no potential to reach the requirements for industrial application as a dense polymer film.[172] Additionally, a method to postsynthetically modify PVDF by a mixture of KOH and $KMnO_4$ in order to effect HF elimination was chosen. During this reaction carbonyl and hydroxyl groups were created in the PVDF structure, which are expected to interact with the amine groups of the NH_2-MIL-53 filler to enhance particle−polymer adhesion and have a positive effect on the separation performance of the MMMs because nonselective voids at the interface are likely to be avoided.[173] The performance of the mixed matrix membranes based on modified PVDF (m-PVDF) MMMs was significantly improved compared with that of unmodified PVDF (Figure 18). The interaction between the modified polymer and the MIL-53 MOFs was studied by tensile tests, IR and DSC measurements and confirmed the formation of hydrogen bonds between the NH_2-groups and carbonyl groups in the material resulted in stronger adhesion with the amine-functionalized filler.

Poly(amide-*b*-ethylene oxide) (Pebax1657, Arkema) is a commercially available PEO/PA copolymer. It is a rubbery

DOI: 10.1021/acs.cgd.7b00595
Cryst. Growth Des. 2017, 17, 4467−4488

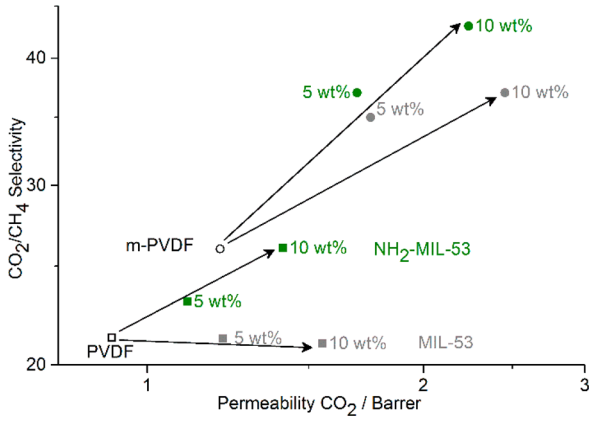

Figure 18. CO_2/CH_4 permselectivity plot for PVDF/MIL-53 MMMs[172] (squares) with standard (gray) and NH_2-MIL-53 (green) for different MOF/MMM mass fractions. With introduction of carbonyl and hydroxyl groups to PVDF the selectivity and permeability of the m-PVDF MMMs[173] (circles) increased due to stronger polymer−filler interaction. See Supporting Information for a graphic and structure description of MIL-53.[149,166,167]

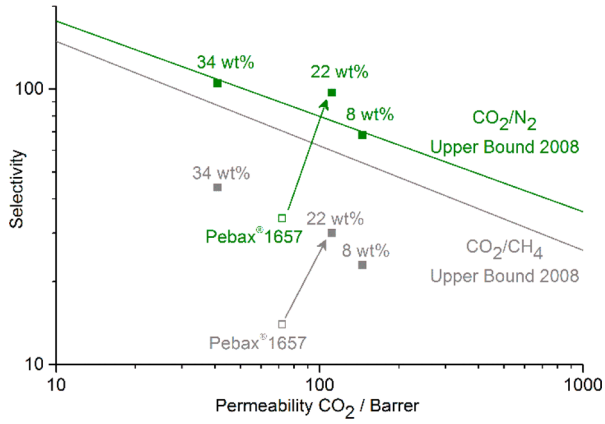

Figure 19. Permeability and selectivity of Pebax1657/ZIF-7 MMMs[175] for different MOF/MMM mass fractions with CO_2/CH_4 (gray) CO_2/N_2 (green) permselectivity. The selective Pebax1657/ZIF-7 layer was deposited on a porous polyacrylonitrile support with a PTMSP gutter layer, with 22 wt % ZIF-7 content in Pebax1657 as the best performing MMMs for both gas pairs. See Supporting Information for a graphic and structure description of ZIF-7.[174]

copolymer that contains poly(ethylene oxide), PEO segments as the permeable phase and a polyamide (PA) crystalline phase that gives mechanical strength to the membrane. With its high chain mobility and functional groups it is expected to have a good interaction with most fillers. Additionally it is easier to prepare defect-free MMMs using low glass transition temperature polymers and rubbery polymers. Using this polymer, thin layers (less than 1 mm) mixed with ZIF-7[174] nanoparticles could be fabricated on a porous poly(acrylonitrile) (PAN) support and these displayed high efficiency in CO_2/CH_4 and CO_2/N_2 separations. An intermediate gutter layer of polytrimethylsilylpropyne (PTMSP) was applied to serve as a flat and smooth surface for coating to avoid polymer penetration into the porous support (it has a very high permeability and does not contribute to the membranes selectivity, because its relative resistance is negligible). Pebax1657 features relatively high CO_2 permeability and a moderate selectivity over N_2 and CH_4. As a MMM with ZIF-7, permeability (up to 145 Barrer for CO_2) and gas selectivity (CO_2/N_2 up to 97 and CO_2/CH_4 up to 30) were increased (Figure 19). The enhanced performance is due to the combination of a molecular sieving effect by the ZIF-7 filler and the high solubility of CO_2 in the polymer.[175]

Further to the introduction of functional groups by chemical modification of the polymer backbone, the possibilities to modify the properties of the polymer matrix are extendable to all areas of polymer chemistry, material science, and plastic processing. One of these techniques is the fabrication of hybrid polymer matrices by mixing a second component into the polymer to gradually influence properties like the thermal stability and flexibility. Additionally, this second component can be incorporated into the space between the filler/polymer phases to interact with both phases. These ternary MMMs can be fabricated as solid/solid-MMMs by using a polymer blend as the matrix or liquid/solid-MMM by mixing with room temperature ionic liquids (RTILs) or low molecular weight polyethyleneglycol (PEG).[176] Ionic liquids were already discussed above as an additive to enhance the CO_2 uptake of the fillers or to tune the pore size of the fillers for controlled sieving effects. ILs can also be blended with polymers as polymeric ionic liquids (PILs). Ionic liquids such as [emim][Ac] are considered good solvents for polysaccharides like chitosan (CS), a biodegradable, biocompatible, nontoxic, and hydrophilic membrane polymer which is a linear polysaccharide obtained by deacetylation of chitin. Excellent solvation of CS is achieved because of strong H-bonds between the acetate anion and the OH groups in the polysaccharide chain.[177] Hybrid solid IL−CS membranes can be prepared by introducing a small amount of [emim][Ac] IL into the CS polymer film.[178] This gave a binary material displaying good adhesion between the components, improved flexibility, as well as a decrease in the influence of temperature on CO_2/N_2 separation. This hybrid matrix was then used to fabricate ternary MMMs with ZIF-8 or HKUST-1 nanoparticles as a porous filler to improve the selectivity of the IL−CS hybrid continuous polymer matrix.[179] The highest CO_2 permeability and CO_2/N_2 ideal selectivity were obtained for 10 wt % ZIF-8 and 5 wt % HKUST-1/IL−CS membranes (5413 Barrer and 11.5, and 4754 Barrer and 19.3, respectively, at 50 °C and 2 bar (Figure 20)). The increase in permselectivity was attributed to the good adhesion and compatibility between the IL, the MOFs and the polymer matrix. For both MOFs, higher or lower loadings gave poorer results. The higher filler loading in the highest performing IL-CS/ZIF-8 MMMs versus IL-CS/HKUST is because of better compatibility between ZIF-8 and the IL.

Polymer properties like plasticization, mechanical stability, and permselectivity can be changed by thermal annealing of the membranes. The polyimide Matrimid, can be cross-linked at high temperatures by annealing. If enough mobility can be obtained through heat treatment, the aromatic imide and phenylene groups in adjacent polymer chains will approach each other closely enough to allow for π-electron interaction, which leads to the formation of charge-transfer complexes. This behavior increases the packing density of the polymer chains and decreases the free volume leading to increased size selectivity in gas separation.[180,181] The influence of the filler in MOF-based MMMs on the annealing of Matrimid was studied by Mahdi et al.[182] evaluating the structure−mechanical property correlations from nanocomposites to a prototypical MOF-polymer MMM composed of Matrimid and ZIF-8 nanoparticles. It was confirmed that the addition of ZIF-8

DOI: 10.1021/acs.cgd.7b00595
Cryst. Growth Des. 2017, 17, 4467−4488

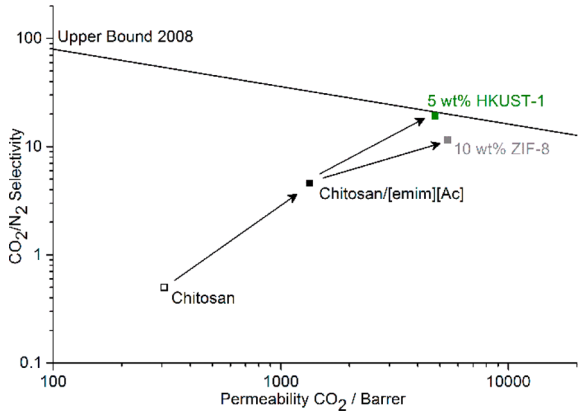

Figure 20. Increase of permeability and selectivity of chitosan-based membranes when [emim][Ac] and MOF fillers are incorporated. The open symbol corresponds to the pure chitosan membrane,[178] closed symbols to the hybrid solid IL−CS membranes[179] with (green) 5 wt % HKUST-1 and (gray) 10 wt % ZIF-8 as the optimum loadings and best performing MMMs with MOF-fillers. See Supporting Information for a graphic and structure description of ZIF-8[131,132] and HKUST-1.[147]

nanoparticles and annealing are both beneficial for gas selectivity. The combination of mechanical characterization and gas separation showed that annealed 10 wt % ZIF-8/Matrimid MMMs would be ideal for practical separation applications because they retained a sizable level of damage tolerance and mechanical robustness, without compromising their toughness relative to annealed neat Matrimid (Figure 21). For the fracture energy and strengths, there is an inverse relation with nanoparticle wt % loading.

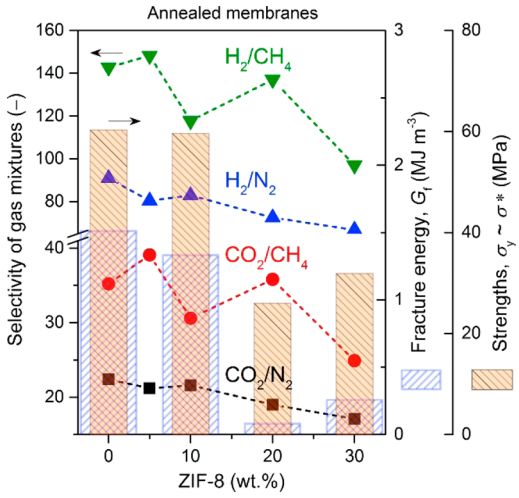

Figure 21. Comparison of the gas selectivity data of annealed Matrimid/ZIF-8 nanocomposite MMMs,[183] versus single gas permeation properties of pure annealed membranes, and the mechanical properties of annealed membranes (fracture energy and strengths). Figure taken from ref 182 with permission. Copyright Elsevier 2016.

2.5. Morphology, Assembly, and Size of Filler Particles. The morphology and size of the filler particles are important properties for the preparation of MOF-MMMs. Predominantly these properties influence the distribution of the filler particles within the polymer matrix and the interactions between filler and matrix. Low degrees of aggregation and smaller particle size are important characteristics of MOF additives for MMMs in order to achieve a uniform distribution of the MOF particles without sedimentation.[45] High filler loadings are desirable to maximize the positive effect of the filler on the polymer matrix. However, there is an optimum loading where a good dispersion of the filler and excellent interfacial contact with the polymer chains result in an optimum MMM performance. At higher loadings often a loss in selectivity is a result of formation of undesirable channels between the particles which aggregate because polymer chains are not able to completely surround and thereby separate the particles anymore.[44] At this optimum loading the permselectivity should be increased with smaller particles because less polymer material is needed to isolate a single particle. Additionally smaller particles are also helpful and essential in the formation of thinner MMMs which have higher permeation rates.[39] Particles in the submicron range have a much better chance of being accommodated inside a thin polymer film or layer, whereby bigger particles risk the formation of pinholes and polymer phase defects.[184] Additionally, with control of the size of MOF particles also the properties and applications are affected.[185] For gas adsorption with MOF nanocrystals not only are the adsorption kinetics improved compared to the bulk material,[186] but also there are cases where the total gas uptake is increased with decreasing particle size.[187,188] This emphasizes the positive effects of using nanosized MOF crystals as filler in MMMs.

Besides other synthesis conditions like pH, solvent, and use of modulators, the heating method in MOF preparation has been extensively shown to be crucial for the resulting morphology and especially for the particle size.[189] For example, the synthesis by microwave (MW) heating has been reported as an effective method to prepare small and uniformly sized MOF particles as suitable fillers for MMMs.[40] The benefit of rapid heating during a microwave-assisted synthesis is that it decreases the particle size of a MOF material in comparison with conventional heating, and commonly a narrower size distribution can be achieved.[190,191] Another example is the sonochemical synthesis of submicron $Zn(pyrz)_2(SiF_6)$[192,193] (also known as SIFSIX-3-Zn[194]) for the preparation of MMMs for CO_2/CH_4 separation.[195] $Zn(pyrz)_2(SiF_6)$ is composed of square grids of Zn and pyrazine pillared by hexafluorosilicate (SiF_6^{2-}) anions, which form one-dimensional channels having a 3.8 Å diagonal dimension.[162] Thus, the material exhibits excellent adsorptive size selectivity of CO_2 over N_2 and CH_4. The bulk material, synthesized by a RT mixing route, with an average particle size of 6 μm, and the submicron sonochemically synthesized $Zn(pyrz)_2(SiF_6)$ particles (average particle size: 860 nm) were comparatively studied as fillers in MMMs with cross-linked poly(ethylene oxide) (XLPEO) as a polymer matrix. The film formation was achieved by radical polymerization of the macro-monomers poly(ethylene glycol) diacrylate and poly(ethylene glycol) methyl ether acrylate using the initiator azobisisobutylonitrile between two glass plates with spacers to get films with well-defined thickness. Gas permeation experiments with CO_2/CH_4 (50/50) binary mixtures as feed gas and incorporation of 10 wt % $Zn(pyrz)_2(SiF_6)$ micrometer (average particle size of 5.7 μm) crystals into the membrane showed an improved separation performance, with CO_2 permeability and CO_2/CH_4 selectivity increased to 540 Barrer and 23, respectively. When 10 wt % $Zn(pyrz)_2(SiF_6)$ submicron crystals were used instead of the larger material, the CO_2 permeability and CO_2/CH_4 selectivity were further enhanced to 620 Barrer and 27, respectively (Figure 22). For CO_2/N_2

DOI: 10.1021/acs.cgd.7b00595
Cryst. Growth Des. 2017, 17, 4467−4488

(20/80) mixtures the same performance trend was observed for the comparison between micrometer and submicron particles as filler material.[195]

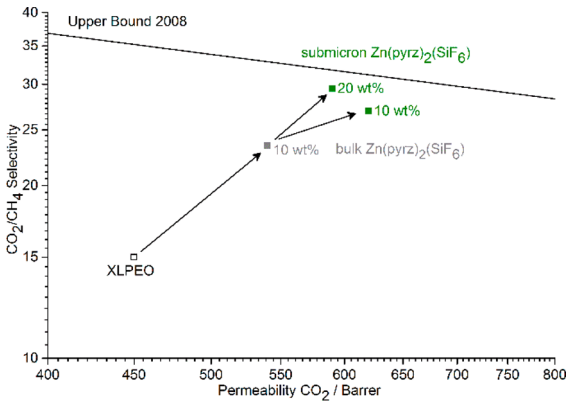

Figure 22. Stepwise increase of permeability and selectivity of cross-linked poly(ethylene oxide) (XLPEO) membranes when Zn-(pyrz)$_2$(SiF$_6$) fillers are incorporated.[195] The open symbol corresponds to the pure polymer membrane, closed symbols to the MMMs with (gray) 10 wt % micrometer Zn(pyrz)$_2$(SiF$_6$) and (green) 10 and 20 wt % submicron Zn(pyrz)$_2$(SiF$_6$) as the optimum loadings and best performing MMMs. See Supporting Information for a graphic and structure description of Zn(pyrz)$_2$(SiF$_6$).[192,193]

Besides variation of the heating method, the use of modulators during the conventional solvothermal synthesis can also facilitate the formation of nanoparticles, suited as a filler for MMMs. (OH)$_2$-UiO-66(Hf) exhibits excellent H_2/CO_2 adsorptive separation performance and can be obtained with nanoparticle morphology when synthesized with acetic acid as a modulator.[196] MMMs containing (OH)$_2$-UiO-66(Hf) nanoparticles dispersed in poly(benzimidazole) (PBI) exhibited excellent H_2/CO_2 separation performance with the potential application in precombustion CO_2 capture.[197] Because of the strong CO_2 adsorption sites and extra free volume contributed by (OH)$_2$-UiO-66(Hf), the MMMs exhibited increased H_2 permeability and H_2/CO_2 selectivity compared to pure PBI membranes. 10 wt % (OH)$_2$-UiO-66(Hf) was found to be the optimum loading with a H_2 permeability of 8 Barrer and H_2/CO_2 selectivity of 19 at 5 bar, which puts it above the 2008 Robeson upper bound (Figure 23).

Another interesting morphological effect (besides the particle size of the filler material) is the form of the MOF particles and has been the subject of recent reviews.[198,199] In the case of the crystal form, crystal morphologies ranging from nanosheets, nanoparticles, and nanorods were comparatively studied. The morphology of MOFs as nanosheets is clearly the optimal particle shape, compared to other nonsheet morphologies.[200−202] Other than the influence of the filler shape on the separation properties of MMMs, the use of hierarchical structured MOF assemblies composed of organized MOF-particles in terms of structure and function also show some interesting recent results on the permeation of MMMs.[203]

MMMs from Matrimid and ZIF-8 were fabricated by a novel approach by using the self-assembly of MOF and polymer particles followed by their controlled fusion to form membranes by DMF vapor annealing. This approach was studied to compare if the separation performance for CO_2/CH_4 gas mixtures of the material can be enhanced when the morphology of the membrane material is optimized and to

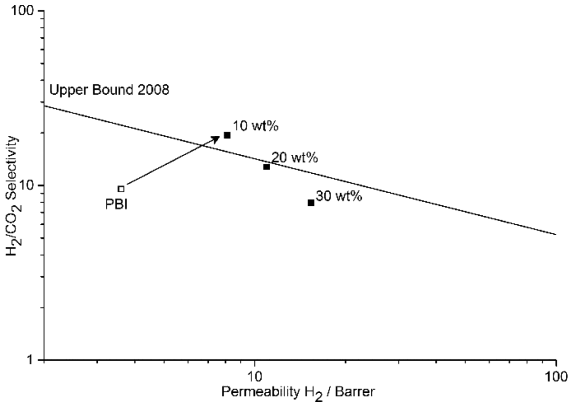

Figure 23. Comparative plot of permeability and selectivity of PBI-based MMMs with different amounts of (OH)$_2$-UiO-66(Hf).[197] The open symbol corresponds to the pure polymer membrane, closed symbols to the MMMs with the arrow indicating the optimum loading at 10 wt % (OH)$_2$-UiO-66(Hf), exceeding the 2008 Robeson upper bound. See Supporting Information for a graphic and structure description of UiO-66.[127,130]

achieve higher filler loadings.[204] The particle fusion approach can be divided into several steps. First, Matrimid polymer particles were prepared whose surface was then modified by the introduction of imidazole groups through grafting of 1-(3-aminopropyl)-imidazole onto the polymer backbone (Figure 24) to enhance the growth of ZIF-8 nanoparticles as a shell with good attachment to these linker groups anchored to the polymer particles. Then dense MMMs were formed in a DMF−vapor environment to induce particle fusion.

Grafted Matrimid MMMs with ZIF-8 loadings up to 30 wt % could be achieved without any loss in selectivity. In the separation of CO_2/CH_4 mixtures the CO_2 permeability increased up to 200% combined with a 65% increase in CO_2/CH_4 selectivity, compared to the native Matrimid. The material also outperforms membranes with the same ZIF-8 loading, prepared without the particle fusion approach, but with an already optimized prime protocol including dispersion and slow evaporation of the solvent (Figure 25).[205] This clearly shows the potential to achieve high performing MMMs with highly compatible, well dispersed and high filler loading when the membrane fabrication technique is optimized in terms of avoiding morphological defects.

Hierarchical structures can also be used to achieve increased permeability when spherical, hollow fillers are incorporated to form extra voids inside of the membrane, and where the sieve particles build a selective shell.[206] With the aim of improving filler−polymer contact, dispersion and gas permeability, hollow ZIF-8 spheres were used as the filler to prepare MMMs containing with the copolymer poly(vinyl chloride)-*g*-poly-(oxyethylene methacrylate) (PVC-*g*-POEM) as the polymer matrix. The hollow MOF-spheres were prepared by solvothermal coating of polystyrene (PS) nanoparticles with ZIF-8, followed by the removal of PS by immersion in DMF. Free standing, defect free MMMs were prepared via a solution casting method with filler loadings up to 30 wt %. SEM-images of the MMMs cross sections show that the hollow MOF-spheres were homogeneously mixed with the PVC-*g*-POEM polymer matrix without any apparent interfacial voids or particle aggregation (Figure 26).

The CO_2/CH_4 gas separation performance of the MMMs was evaluated by pure gas permeation measurements at 35 °C.

DOI: 10.1021/acs.cgd.7b00595
Cryst. Growth Des. 2017, 17, 4467−4488

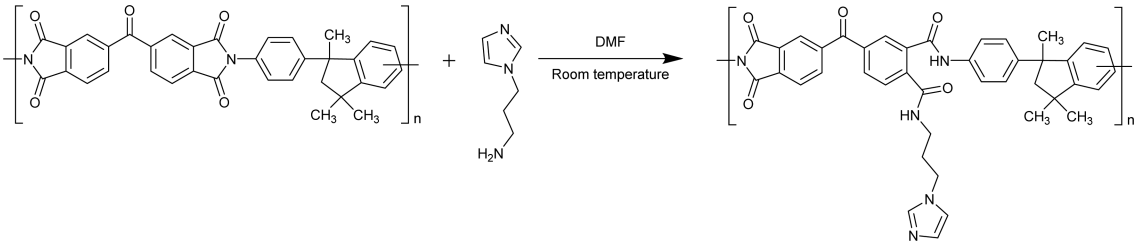

Figure 24. Grafting of 1-(3-aminopropyl)-imidazole on Matrimid.

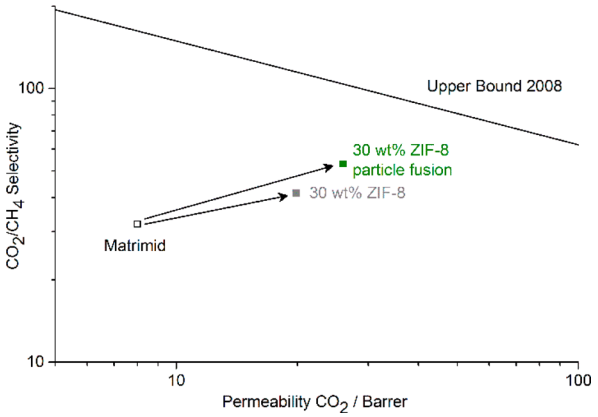

Figure 25. Permeability and selectivity of a 30 wt % Matrimid/ZIF-8 MMM[205] (gray) and increased permselectivity for a Matrimid/ZIF-8 MMM prepared by particle fusion and the same amount of ZIF-8[204] (green). See Supporting Information for a graphic and structure description of ZIF-8.[131,132]

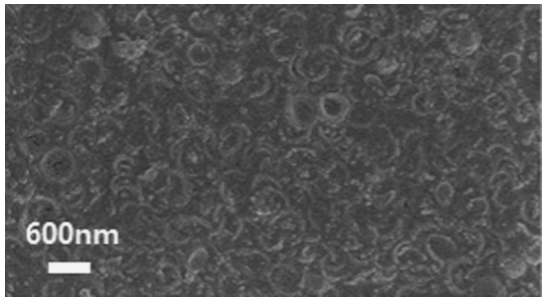

Figure 26. SEM image of the cross section of a 30 wt % PVC-*g*-POEM/hollow ZIF-8 sphere MMM. Figure adapted from ref 206 with permission. Copyright Elsevier 2015.

For MMMs with 30 wt % ZIF-8 the CO_2 permeability increased from 70 Barrer for neat PVC-*g*-POEM membranes to 623 Barrer with a slight loss in selectivity from 14 to 11 (Figure 27). ZIF-8 has the potential to have a molecular sieving effect as a filler in MMMs. The loss in selectivity for PVC-*g*-POEM/ZIF-8 MMMs may be due to the effect that the walls of the hollow spheres do not consist of completely intergrown ZIF-8 particles. In this case, cracks or holes between the crystals show no resistance to the passage of both gases creating nonselective areas inside the spheres and thereby decreasing the selectivity of the MMM.

3. CONCLUSIONS AND OUTLOOK

The combination of MOFs and polymers to fabricate MMMs is a promising strategy to avoid the trade-off between permeability and selectivity for organic polymers and to realize materials with separation properties exceeding the Robeson

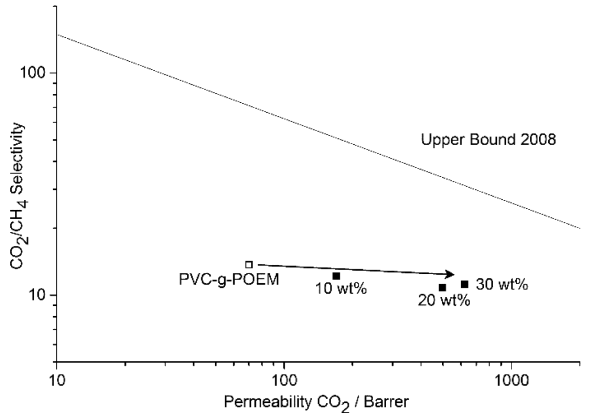

Figure 27. Effect of increased permeability on PVC-*g*-POEM/ZIF-8 MMMs[206] with increasing filler loading when ZIF-8 is fabricated as a hollow sphere before incorporation into the MMM in order to create extra voids with higher permeation compared to the dense material. See Supporting Information for a graphic and structure description of ZIF-8.[131,132]

upper bound, reaching the potential for industrial application. Most work focuses on the separation of CO_2/CH_4 for natural gas sweetening or CO_2/N_2 separation for the purification of flue gases (cf. Table 1). In summary, all described MMMs exhibited enhanced separation performance depending on optimal filler loading and membrane integrity at high filler loadings or enhanced filler performance.

Permeation data for the MMMs presented in this review is collated in Table 1. These data were collected from studies which use a variety of characterization methods for gas separation and variable, but similar measurement conditions, at temperatures ranging from 25 to 50 °C and transmembrane pressures between 1 and 10 bar. As a consequence, this overview adds to the systematic comparison of the pure polymer material and the effect of the presented MOF fillers on permeability and selectivity presented throughout the review. For better comparison "round robin" tests under very similar conditions, including three different laboratories, have been already reported by Sanchez-Lainez et al. for ZIF-8 MMMs.[207] The "round robin" study showed exemplary reproducibility of the membrane permeation analysis methodology by tests involving different European universities (UNIZAR from Zaragoza, Spain, LUH from Hannover, Germany, and TUDelft from Delft, The Netherlands).

It should be emphasized that more studies like this which employ identical conditions for testing gas permeation under industrially relevant conditions should be developed. Particularly, mixed gas permeation and the influence of contaminants on the separation performance should be quantified. This is illustrated for the case of SPEEK in the combination of sulfonated MIL-101(Cr)[111] or with functionalized PEI@MIL-

DOI: 10.1021/acs.cgd.7b00595
Cryst. Growth Des. 2017, 17, 4467−4488

101[143] as a filler. The presence of water as a contaminant in the gas stream enabled and reinforced facilitated transport for CO_2 through the MMM material, thereby drastically enhancing the selectivity and permeability at 40 wt % loading in the separation of a CO_2/CH_4 gas mixture beyond the upper bound.

The discussed methods to tailor the MMM properties especially showed great effects in the case, where a combination of a filler with designed pore size by IL incorporation ([bmim][Tf_2N]@ZIF-8) and a asymmetric MMM with a very thin selective PSF/MOF layer was utilized for the separation of a CO_2/N_2 gas mixture.[136] Both the excellent size selective pores of the modified filler, which resulted in enhanced selectivity, and the increased permeation rate of the thin MMM, resulted in a gas separation performance surpassing the Robeson upper bound. In a similar way a high separation performance of a CO_2/N_2 gas mixture was achieved for Pebax1657 MMMs with ZIF-7 nanoparticles as a filler. At 22 wt % loading the thin selective MMM layer, supported by a porous poly(acrylonitrile) support with a PTMSP gutter layer, was still intact due to the homogeneous dispersion of the ZIF-7 nanoparticles in the MMM (Figure 28).[175]

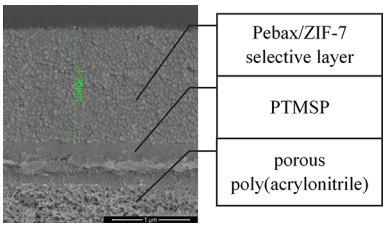

Figure 28. SEM cross-section of a composite membrane with (from top to bottom) selective MMM layer of Pebax1657 with 34 wt % ZIF-7, PTMSP gutter layer and porous poly(acrylonitrile) support as representation of an asymmetric membrane. The scale bar is 1 μm. Figure adapted from ref 175 with permission. Copyright Elsevier 2013.

In a similar manner recent research on hollow fiber MOF MMMs have shown interesting results pointing the way to the industrial future of MOF based membranes and providing the possibility for MOF membranes to be industrially viable products for separations.[63] Koros et al. have incorporated ZIF-8 into an Ultem matrix and produced dual layer asymmetric hollow fiber membranes. The fibers showed increased permselectivity enhancements as high as 20% over the pure polymer.[47] Another approach is the coating of asymmetric hollow fiber membranes from PSF with a PDMS solution containing suspended HKUST-1 by a dip-coating technique.[62] Continuous, that is, pure MOF, membranes inside polymer hollow fibers could be synthesized by a microfluidic approach. Nair et al. have fabricated continuous molecular sieving ZIF-8 membranes in poly(amide-imide) hollow fibers, with H_2/C_3H_8 and C_3H_6/C_3H_8 separation factors as high as 370 and 12.[208] The key challenge in the synthesis of continuous MOF membranes is the control over the crystal growth position on the fiber and could be managed by a room temperature interfacial method for growing MOFs (ZIF-8 and HKUST-1) on either the outer or inner side of a polybenzimidazole-based hollow fiber (PBI-BuI-HF) membrane surface.[209] Coronas et al. have successfully expanded the microfluidic approach to a variety of continuous MOF membranes. Microfluidics provides a constant reactant concentration along the membrane for growing homogeneous, continuous and thin MOF layers. ZIF-93 continuous membranes were synthesized on the inner side of P84 copolyimide hollow fiber supports, and high selectivities in the separation of H_2/CH_4 (59.7) and CO_2/CH_4 (16.9) mixtures were obtained.[210] ZIF-7 and ZIF-8 membranes were synthesized on the inner surface of a polysulfone hollow fiber.[211] The separation performance of ZIF-8 and ZIF-93 membranes can be further enhanced when grown inside of a copolyimide P84 hollow fiber together with in situ thermal annealing. Gas separation selectivity increased without any significant reduction in the gas permeance, and H_2/CH_4 and CO_2/CH_4 selectivities of 103 and 18 (ZIF-8) and 101 and 20 (ZIF-93) were obtained.[212]

These results demonstrate the importance of membrane fabrication in respect to module geometries suited for industrial large scale separation processes, where the productivity of a membrane is increased by the usage of asymmetric membranes. With selective layers, lower than 1 μm, the performance of low flux polymers like PSF can be enhanced to move the separation properties to a commercially interesting area, as mentioned above. Thereby strategies like modulation of the MOF synthesis and control of the particle size are powerful tools to design additives for high performing MMMs. The fine-tuning of the MMM properties by utilization of the chemical functionality of the MOF linker,[108] or by introduction of functional groups by post synthetic modification,[123,129] and also the design of new polyMOFs[153,158,159] which, while creating a new subclass of MOF materials with a great potential for being high performing membranes for gas separation, confirms that the high expectations of MOFs as multifunctional organic–inorganic hybrid materials are being successfully fulfilled. The high versatility of MOF chemistry enables the research community to target interesting effects, like the usage of the chemical modifications to not only increase the performance for a specific application, but also to increase the stability, which is an important step in making industrial applications possible.[213]

■ ASSOCIATED CONTENT

Supporting Information

The Supporting Information is available free of charge on the ACS Publications website at DOI: 10.1021/acs.cgd.7b00595.

Brief mathematical description of permeability and selectivity; graphical representations and brief structure descriptions of MOFs given in the main text (PDF)

■ AUTHOR INFORMATION

Corresponding Authors

*(C.J.) E-mail: janiak@uni-duesseldorf.de.
*(C.J.S.) E-mail: christopher.sumby@adelaide.edu.au.

ORCID

Christoph Janiak: 0000-0002-6288-9605

Notes

The authors declare no competing financial interest.

■ ACKNOWLEDGMENTS

C.J.S. acknowledges the Australian Research Council and the University of Adelaide, the latter for funding the visit of C.J. C.J. thanks the DFG for support through Grant Ja466/29-1 and the Anton-Betz foundation.

DOI: 10.1021/acs.cgd.7b00595
Cryst. Growth Des. 2017, 17, 4467–4488

ABBREVIATIONS

single const. vol., single gas, constant volume method; single const. pres., single gas, constant pressure method; mixed const. vol., mixed gas, constant volume method; mixed const. pres., mixed gas, constant pressure method; mixed sweep, sweep gas method (see section 1.1, and Supporting Information for further information)

REFERENCES

(1) Abetz, V.; Brinkmann, T.; Dijkstra, M.; Ebert, K.; Fritsch, D.; Ohlrogge, K.; Paul, D.; Peinemann, K. V.; Pereira-Nunes, S.; Scharnagl, N.; Schossig, M. *Adv. Eng. Mater.* **2006**, *8*, 328−358.
(2) Koros, W. J.; Mahajan, R. *J. Membr. Sci.* **2000**, *175*, 181−196.
(3) Davis, J.; Valus, R.; Eshraghi, R.; Velikoff, A. *Sep. Sci. Technol.* **1993**, *28*, 463−476.
(4) Buonomenna, M. G. *RSC Adv.* **2013**, *3*, 5694−5740.
(5) He, X.; Hägg, M.-B. *Membranes* **2012**, *2*, 706−726.
(6) Ohlrogge, K.; Stürken, K. The Separation of Organic Vapors from Gas Streams by Means of Membranes. In *Membrane Technology*; Wiley-VCH Verlag GmbH, 2001; pp 69−94.
(7) Baker, R. W. *Ind. Eng. Chem. Res.* **2002**, *41*, 1393−1411.
(8) BORSIG Membrane Technology GmbH. http://www.borsig-china.com/#productrecovery (accessed 2016).
(9) Sulzer Chemtech AG. http://www.sulzer.com/en/Products-and-Services/Separation-Technology/Membrane-Technology/Organic-Solvent-Nanofiltration-OSN (accessed 2016).
(10) Wiederhorn, S.; Fields, R.; Low, S.; Bahng, G.-W.; Wehrstedt, A.; Hahn, J.; Tomota, Y.; Miyata, T.; Lin, H.; Freeman, B.; Aihara, S.; Hagihara, Y.; Tagawa, T. Mechanical Properties. In *Springer Handbook of Materials Measurement Methods*; Czichos, H.; Saito, T.; Smith, L., Eds.; Springer: Berlin, Heidelberg, 2006; Chapter 7, pp 283−397.
(11) Dong, G.; Li, H.; Chen, V. *J. Membr. Sci.* **2011**, *369*, 206−220.
(12) Merkel, T. C.; Lin, H.; Wei, X.; Baker, R. *J. Membr. Sci.* **2010**, *359*, 126−139.
(13) Huang, Y.; Merkel, T. C.; Baker, R. W. *J. Membr. Sci.* **2014**, *463*, 33−40.
(14) IEA Bioenergy. http://www.iea-biogas.net/files/daten-redaktion/download/publi-task37/Biogas%20upgrading.pdf (accessed 2016).
(15) Basu, S.; Khan, A. L.; Cano-Odena, A.; Liu, C.; Vankelecom, I. F. J. *Chem. Soc. Rev.* **2010**, *39*, 750−768.
(16) Wind, J. D.; Staudt-Bickel, C.; Paul, D. R.; Koros, W. J. *Ind. Eng. Chem. Res.* **2002**, *41*, 6139−6148.
(17) Robeson, L. M. *J. Membr. Sci.* **1991**, *62*, 165−185.
(18) Robeson, L. M. *J. Membr. Sci.* **2008**, *320*, 390−400.
(19) Jessie Lue, S.; Peng, S. H. *J. Membr. Sci.* **2003**, *222*, 203−217.
(20) Qiu, S.; Ben, T. In *Porous polymers: Design, Synthesis and Applications*; RSC Publishing: Cambridge, 2015.
(21) Davis, M. E. *Ind. Eng. Chem. Res.* **1991**, *30*, 1675−1683.
(22) Liu, J.; Yu, J. Chapter 1 - Toward Greener and Designed Synthesis of Zeolite Materials A2 - Sels, Bert F. In *Zeolites and Zeolite-Like Materials*; Kustov, L. M., Ed.; Elsevier: Amsterdam, 2016; pp 1−32.
(23) Furukawa, H.; Cordova, K. E.; O'Keeffe, M.; Yaghi, O. M. *Science* **2013**, *341*, 1230444−1−12.
(24) Ryoo, R.; Joo, S. H.; Jun, S. *J. Phys. Chem. B* **1999**, *103*, 7743−7746.
(25) Davis, M. E. *Nature* **2002**, *417*, 813−821.
(26) Harris, P. J. F. In *Carbon Nanotube Science: Synthesis, Properties and Applications*; Cambridge University Press, 2009.
(27) Jiang, L.; Fan, Z. *Nanoscale* **2014**, *6*, 1922−1945.
(28) Tanh Jeazet, H. B.; Staudt, C.; Janiak, C. *Dalton Trans.* **2012**, *41*, 14003−14027.
(29) Caro, J.; Noack, M. *Microporous Mesoporous Mater.* **2008**, *115*, 215−233.
(30) Caro, J.; Noack, M.; Kölsch, P.; Schäfer, R. *Microporous Mesoporous Mater.* **2000**, *38*, 3−24.
(31) Rangnekar, N.; Mittal, N.; Elyassi, B.; Caro, J.; Tsapatsis, M. *Chem. Soc. Rev.* **2015**, *44*, 7128−7154.
(32) Li, W.; Zhang, Y.; Li, Q.; Zhang, G. *Chem. Eng. Sci.* **2015**, *135*, 232−257.
(33) Bux, H.; Chmelik, C.; Krishna, R.; Caro, J. *J. Membr. Sci.* **2011**, *369*, 284−289.
(34) Li, Y.-S.; Liang, F.-Y.; Bux, H.; Feldhoff, A.; Yang, W.-S.; Caro, J. *Angew. Chem.* **2010**, *122*, 558−561.
(35) Bastani, D.; Esmaeili, N.; Asadollahi, M. *J. Ind. Eng. Chem.* **2013**, *19*, 375−393.
(36) Lai, Z.; Bonilla, G.; Diaz, I.; Nery, J. G.; Sujaoti, K.; Amat, M. A.; Kokkoli, E.; Terasaki, O.; Thompson, R. W.; Tsapatsis, M.; Vlachos, D. G. *Science* **2003**, *300*, 456−460.
(37) Venna, S. R.; Carreon, M. A. *Chem. Eng. Sci.* **2015**, *124*, 3−19.
(38) Zhang, Y.; Feng, X.; Yuan, S.; Zhou, J.; Wang, B. *Inorg. Chem. Front.* **2016**, *3*, 896−909.
(39) Chung, T.-S.; Jiang, L. Y.; Li, Y.; Kulprathipanja, S. *Prog. Polym. Sci.* **2007**, *32*, 483−507.
(40) Zornoza, B.; Martinez-Joaristi, A.; Serra-Crespo, P.; Téllez, C.; Coronas, J.; Gascon, J.; Kapteijn, F. *Chem. Commun.* **2011**, *47*, 9522−9524.
(41) Nik, O. G.; Chen, X. Y.; Kaliaguine, S. *J. Membr. Sci.* **2012**, *413−414*, 48−61.
(42) Hunger, K.; Schmeling, N.; Jeazet, H. B.; Janiak, C.; Staudt, C.; Kleinermanns, K. *Membranes* **2012**, *2*, 727−763.
(43) Jeazet, H. B. T.; Janiak, C. Metal-Organic Frameworks in Mixed-Matrix Membranes. In *Metal-Organic Framework Materials*; MacGillivray, L. R.; Lukehart, C., Eds.; John Wiley & Sons, Ltd: Chichester, 2014; pp 1−15.
(44) Zornoza, B.; Téllez, C.; Coronas, J.; Gascon, J.; Kapteijn, F. *Microporous Mesoporous Mater.* **2013**, *166*, 67−78.
(45) Dong, G.; Li, H.; Chen, V. *J. Mater. Chem. A* **2013**, *1*, 4610−4630.
(46) Ordoñez, M. J. C.; Balkus, K. J., Jr; Ferraris, J. P.; Musselman, I. H. *J. Membr. Sci.* **2010**, *361*, 28−37.
(47) Dai, Y.; Johnson, J. R.; Karvan, O.; Sholl, D. S.; Koros, W. J. *J. Membr. Sci.* **2012**, *401−402*, 76−82.
(48) Zheng, D.; Liu, X.; Hu, D.; Li, M.; Zhang, J.; Zeng, G.; Zhang, Y.; Sun, Y. *RSC Adv.* **2014**, *4*, 10140−10143.
(49) Buonomenna, M. G.; Yave, W.; Golemme, G. *RSC Adv.* **2012**, *2*, 10745−10773.
(50) Chen, X. Y.; Vinh-Thang, H.; Rodrigue, D.; Kaliaguine, S. *RSC Adv.* **2014**, *4*, 12235−12244.
(51) Sorribas, S.; Zornoza, B.; Téllez, C.; Coronas, J. *J. Membr. Sci.* **2014**, *452*, 184−192.
(52) Burmann, P.; Zornoza, B.; Téllez, C.; Coronas, J. *Chem. Eng. Sci.* **2014**, *107*, 66−75.
(53) Chen, X. Y.; Vinh-Thang, H.; Rodrigue, D.; Kaliaguine, S. *Ind. Eng. Chem. Res.* **2012**, *51*, 6895−6906.
(54) Seoane, B.; Zamaro, J. M.; Tellez, C.; Coronas, J. *RSC Adv.* **2011**, *1*, 917−922.
(55) Chen, X. Y.; Hoang, V.-T.; Rodrigue, D.; Kaliaguine, S. *RSC Adv.* **2013**, *3*, 24266−24279.
(56) Rebollar-Perez, G.; Carretier, E.; Lesage, N.; Moulin, P. *Membranes* **2011**, *1*, 80−90.
(57) Dumee, L.; Velleman, L.; Sears, K.; Hill, M.; Schutz, J.; Finn, N.; Duke, M.; Gray, S. *Membranes* **2011**, *1*, 25−36.
(58) Baker, R. W.; Lokhandwala, K. *Ind. Eng. Chem. Res.* **2008**, *47*, 2109−2121.
(59) Basu, S.; Cano-Odena, A.; Vankelecom, I. F. J. *J. Membr. Sci.* **2010**, *362*, 478−487.
(60) Wijenayake, S. N.; Panapitiya, N. P.; Versteeg, S. H.; Nguyen, C. N.; Goel, S.; Balkus, K. J.; Musselman, I. H.; Ferraris, J. P. *Ind. Eng. Chem. Res.* **2013**, *52*, 6991−7001.
(61) Wijenayake, S. N.; Panapitiya, N. P.; Nguyen, C. N.; Huang, Y.; Balkus, K. J., Jr; Musselman, I. H.; Ferraris, J. P. *Sep. Purif. Technol.* **2014**, *135*, 190−198.
(62) Zulhairun, A. K.; Fachrurrazi, Z. G.; Nur Izwanne, M.; Ismail, A. F. *Sep. Purif. Technol.* **2015**, *146*, 85−93.

DOI: 10.1021/acs.cgd.7b00595
Cryst. Growth Des. 2017, 17, 4467−4488

(63) Hu, J.; Cai, H.; Ren, H.; Wei, Y.; Xu, Z.; Liu, H.; Hu, Y. *Ind. Eng. Chem. Res.* **2010**, *49*, 12605−12612.
(64) Seoane, B.; Coronas, J.; Gascon, I.; Benavides, M. E.; Karvan, O.; Caro, J.; Kapteijn, F.; Gascon, J. *Chem. Soc. Rev.* **2015**, *44*, 2421−2454.
(65) Noble, R. D. *J. Membr. Sci.* **2011**, *378*, 393−397.
(66) Li, J.-R.; Ma, Y.; McCarthy, M. C.; Sculley, J.; Yu, J.; Jeong, H.-K.; Balbuena, P. B.; Zhou, H.-C. *Coord. Chem. Rev.* **2011**, *255*, 1791−1823.
(67) Liu, D.; Zhong, C. *J. Mater. Chem.* **2010**, *20*, 10308−10318.
(68) Meek, S. T.; Greathouse, J. A.; Allendorf, M. D. *Adv. Mater.* **2011**, *23*, 249−267.
(69) Bae, T. H.; Lee, J. S.; Qiu, W.; Koros, W. J.; Jones, C. W.; Nair, S. *Angew. Chem., Int. Ed.* **2010**, *49*, 9863−9866.
(70) Janiak, C.; Vieth, J. K. *New J. Chem.* **2010**, *34*, 2366−2388.
(71) Czaja, A. U.; Trukhan, N.; Muller, U. *Chem. Soc. Rev.* **2009**, *38*, 1284−1293.
(72) Bloch, E. D.; Queen, W. L.; Krishna, R.; Zadrozny, J. M.; Brown, C. M.; Long, J. R. *Science* **2012**, *335*, 1606−1610.
(73) Chen, B.; Ockwig, N. W.; Millward, A. R.; Contreras, D. S.; Yaghi, O. M. *Angew. Chem., Int. Ed.* **2005**, *44*, 4745−4749.
(74) Mueller, U.; Schubert, M.; Teich, F.; Puetter, H.; Schierle-Arndt, K.; Pastre, J. *J. Mater. Chem.* **2006**, *16*, 626−636.
(75) Li, Y.; Yang, W. *J. Membr. Sci.* **2008**, *316*, 3−17.
(76) Bowen, T. C.; Noble, R. D.; Falconer, J. L. *J. Membr. Sci.* **2004**, *245*, 1−33.
(77) Kosinov, N.; Gascon, J.; Kapteijn, F.; Hensen, E. J. M. *J. Membr. Sci.* **2016**, *499*, 65−79.
(78) NGK INSULATORS, LTD., http://www.ngk.co.jp/english/research/ecology.html (accessed 2016).
(79) Pera-Titus, M. *Chem. Rev.* **2014**, *114*, 1413−1492.
(80) Chen, Y. F.; Babarao, R.; Sandler, S. I.; Jiang, J. W. *Langmuir* **2010**, *26*, 8743−8750.
(81) Denny, M. S., Jr; Moreton, J. C.; Benz, L.; Cohen, S. M. *Nat. Rev. Mater.* **2016**, *1*, 16078.
(82) Jia, Z.; Wu, G. *Microporous Mesoporous Mater.* **2016**, *235*, 151−159.
(83) Sorribas, S.; Gorgojo, P.; Téllez, C.; Coronas, J.; Livingston, A. G. *J. Am. Chem. Soc.* **2013**, *135*, 15201−15208.
(84) Echaide-Gorriz, C.; Navarro, M.; Téllez, C.; Coronas, J. *Dalton Trans.* **2017**, *46*, 6244−6252.
(85) Sorribas, S.; Kudasheva, A.; Almendro, E.; Zornoza, B.; de la Iglesia, Ó.; Téllez, C.; Coronas, J. *Chem. Eng. Sci.* **2015**, *124*, 37−44.
(86) Low, J. J.; Benin, A. I.; Jakubczak, P.; Abrahamian, J. F.; Faheem, S. A.; Willis, R. R. *J. Am. Chem. Soc.* **2009**, *131*, 15834−15842.
(87) Leus, K.; Bogaerts, T.; De Decker, J.; Depauw, H.; Hendrickx, K.; Vrielinck, H.; Van Speybroeck, V.; Van Der Voort, P. *Microporous Mesoporous Mater.* **2016**, *226*, 110−116.
(88) Jeremias, F.; Fröhlich, D.; Janiak, C.; Henninger, S. K. *New J. Chem.* **2014**, *38*, 1846−1852.
(89) Jeremias, F.; Fröhlich, D.; Janiak, C.; Henninger, S. K. *RSC Adv.* **2014**, *4*, 24073−24082.
(90) Janiak, C.; Henninger, S. K. *Chimia* **2013**, *67*, 419−424.
(91) Férey, G.; Mellot-Draznieks, C.; Serre, C.; Millange, F.; Dutour, J.; Surblé, S.; Margiolaki, I. *Science* **2005**, *309*, 2040−2042.
(92) Ehrenmann, J.; Henninger, S. K.; Janiak, C. *Eur. J. Inorg. Chem.* **2011**, *2011*, 471−474.
(93) Khutia, A.; Rammelberg, H. U.; Schmidt, T.; Henninger, S.; Janiak, C. *Chem. Mater.* **2013**, *25*, 790−798.
(94) Karmakar, S.; Dechnik, J.; Janiak, C.; De, S. *J. Hazard. Mater.* **2016**, *303*, 10−20.
(95) Fröhlich, D.; Henninger, S. K.; Janiak, C. *Dalton Trans.* **2014**, *43*, 15300−15304.
(96) Küsgens, P.; Rose, M.; Senkovska, I.; Fröde, H.; Henschel, A.; Siegle, S.; Kaskel, S. *Microporous Mesoporous Mater.* **2009**, *120*, 325−330.
(97) Wu, T.; Shen, L.; Luebbers, M.; Hu, C.; Chen, Q.; Ni, Z.; Masel, R. I. *Chem. Commun.* **2010**, *46*, 6120−6122.
(98) DeCoste, J. B.; Peterson, G. W. *Chem. Rev.* **2014**, *114*, 5695−5727.
(99) Vellingiri, K.; Deep, A.; Kim, K.-H. *ACS Appl. Mater. Interfaces* **2016**, *8*, 29835−29857.
(100) Cmarik, G. E.; Kim, M.; Cohen, S. M.; Walton, K. S. *Langmuir* **2012**, *28*, 15606−15613.
(101) Dan-Hardi, M.; Serre, C.; Frot, T.; Rozes, L.; Maurin, G.; Sanchez, C.; Férey, G. *J. Am. Chem. Soc.* **2009**, *131*, 10857−10859.
(102) Zlotea, C.; Phanon, D.; Mazaj, M.; Heurtaux, D.; Guillerm, V.; Serre, C.; Horcajada, P.; Devic, T.; Magnier, E.; Cuevas, F.; Ferey, G.; Llewellyn, P. L.; Latroche, M. *Dalton Trans.* **2011**, *40*, 4879−4881.
(103) Goesten, M. G.; Juan-Alcañiz, J.; Ramos-Fernandez, E. V.; Sai Sankar Gupta, K. B.; Stavitski, E.; van Bekkum, H.; Gascon, J.; Kapteijn, F. *J. Catal.* **2011**, *281*, 177−187.
(104) Torrisi, A.; Mellot-Draznieks, C.; Bell, R. G. *J. Chem. Phys.* **2010**, *132*, 044705−1−13.
(105) Seoane, B.; Téllez, C.; Coronas, J.; Staudt, C. *Sep. Purif. Technol.* **2013**, *111*, 72−81.
(106) Rodenas, T.; van Dalen, M.; Serra-Crespo, P.; Kapteijn, F.; Gascon, J. *Microporous Mesoporous Mater.* **2014**, *192*, 35−42.
(107) Guo, X.; Huang, H.; Ban, Y.; Yang, Q.; Xiao, Y.; Li, Y.; Yang, W.; Zhong, C. *J. Membr. Sci.* **2015**, *478*, 130−139.
(108) Waqas Anjum, M.; Bueken, B.; De Vos, D.; Vankelecom, I. F. J. *J. Membr. Sci.* **2016**, *502*, 21−28.
(109) Vanherck, K.; Vandezande, P.; Aldea, S. O.; Vankelecom, I. F. J. *J. Membr. Sci.* **2008**, *320*, 468−476.
(110) Li, Z.; He, G.; Zhao, Y.; Cao, Y.; Wu, H.; Li, Y.; Jiang, Z. *J. Power Sources* **2014**, *262*, 372−379.
(111) Xin, Q.; Liu, T.; Li, Z.; Wang, S.; Li, Y.; Li, Z.; Ouyang, J.; Jiang, Z.; Wu, H. *J. Membr. Sci.* **2015**, *488*, 67−78.
(112) Sijbesma, H.; Nymeijer, K.; van Marwijk, R.; Heijboer, R.; Potreck, J.; Wessling, M. *J. Membr. Sci.* **2008**, *313*, 263−276.
(113) Xin, Q.; Wu, H.; Jiang, Z.; Li, Y.; Wang, S.; Li, Q.; Li, X.; Lu, X.; Cao, X.; Yang, J. *J. Membr. Sci.* **2014**, *467*, 23−35.
(114) Denny, M. S.; Cohen, S. M. *Angew. Chem., Int. Ed.* **2015**, *54*, 9029−9032.
(115) Luan, Y.; Qi, Y.; Gao, H.; Andriamitantsoa, R. S.; Zheng, N.; Wang, G. *J. Mater. Chem. A* **2015**, *3*, 17320−17331.
(116) Wang, Z.; Cohen, S. M. *Chem. Soc. Rev.* **2009**, *38*, 1315−1329.
(117) Yi, X.-C.; Xi, F.-G.; Qi, Y.; Gao, E.-Q. *RSC Adv.* **2015**, *5*, 893−900.
(118) Fei, H.; Pullen, S.; Wagner, A.; Ott, S.; Cohen, S. M. *Chem. Commun.* **2015**, *51*, 66−69.
(119) Karagiaridi, O.; Vermeulen, N. A.; Klet, R. C.; Wang, T. C.; Moghadam, P. Z.; Al-Juaid, S. S.; Stoddart, J. F.; Hupp, J. T.; Farha, O. K. *Inorg. Chem.* **2015**, *54*, 1785−1790.
(120) Song, Y.-F.; Cronin, L. *Angew. Chem., Int. Ed.* **2008**, *47*, 4635−4637.
(121) Tanabe, K. K.; Cohen, S. M. *Chem. Soc. Rev.* **2011**, *40*, 498−519.
(122) Cohen, S. M. *Chem. Rev.* **2012**, *112*, 970−1000.
(123) Venna, S. R.; Lartey, M.; Li, T.; Spore, A.; Kumar, S.; Nulwala, H. B.; Luebke, D. R.; Rosi, N. L.; Albenze, E. *J. Mater. Chem. A* **2015**, *3*, 5014−5022.
(124) Schaate, A.; Roy, P.; Godt, A.; Lippke, J.; Waltz, F.; Wiebcke, M.; Behrens, P. *Chem. - Eur. J.* **2011**, *17*, 6643−6651.
(125) Liu, Q.; Jin, L.-N.; Sun, W.-Y. *CrystEngComm* **2013**, *15*, 8250−8254.
(126) Wißmann, G.; Schaate, A.; Lilienthal, S.; Bremer, I.; Schneider, A. M.; Behrens, P. *Microporous Mesoporous Mater.* **2012**, *152*, 64−70.
(127) Valenzano, L.; Civalleri, B.; Chavan, S.; Bordiga, S.; Nilsen, M. H.; Jakobsen, S.; Lillerud, K. P.; Lamberti, C. *Chem. Mater.* **2011**, *23*, 1700−1718.
(128) Vermoortele, F.; Bueken, B.; Le Bars, G.; Van de Voorde, B.; Vandichel, M.; Houthoofd, K.; Vimont, A.; Daturi, M.; Waroquier, M.; Van Speybroeck, V.; Kirschhock, C.; De Vos, D. E. *J. Am. Chem. Soc.* **2013**, *135*, 11465−11468.

DOI: 10.1021/acs.cgd.7b00595
Cryst. Growth Des. 2017, 17, 4467−4488

(129) Anjum, M. W.; Vermoortele, F.; Khan, A. L.; Bueken, B.; De Vos, D. E.; Vankelecom, I. F. J. *ACS Appl. Mater. Interfaces* **2015**, *7*, 25193−25201.
(130) Cavka, J. H.; Jakobsen, S.; Olsbye, U.; Guillou, N.; Lamberti, C.; Bordiga, S.; Lillerud, K. P. *J. Am. Chem. Soc.* **2008**, *130*, 13850−13851.
(131) Huang, X.-C.; Lin, Y.-Y.; Zhang, J.-P.; Chen, X.-M. *Angew. Chem.* **2006**, *118*, 1587−1589.
(132) Park, K. S.; Ni, Z.; Côté, A. P.; Choi, J. Y.; Huang, R.; Uribe-Romo, F. J.; Chae, H. K.; O'Keeffe, M.; Yaghi, O. M. *Proc. Natl. Acad. Sci. U. S. A.* **2006**, *103*, 10186−10191.
(133) Bux, H.; Liang, F.; Li, Y.; Cravillon, J.; Wiebcke, M.; Caro, J. *J. Am. Chem. Soc.* **2009**, *131*, 16000−16001.
(134) Fairen-Jimenez, D.; Moggach, S. A.; Wharmby, M. T.; Wright, P. A.; Parsons, S.; Düren, T. *J. Am. Chem. Soc.* **2011**, *133*, 8900−8902.
(135) Novaković, S. B.; Bogdanović, G. A.; Heering, C.; Makhloufi, G.; Francuski, D.; Janiak, C. *Inorg. Chem.* **2015**, *54*, 2660−2670.
(136) Ban, Y.; Li, Z.; Li, Y.; Peng, Y.; Jin, H.; Jiao, W.; Guo, A.; Wang, P.; Yang, Q.; Zhong, C.; Yang, W. *Angew. Chem.* **2015**, *127*, 15703−15707.
(137) Hasib-ur-Rahman, M.; Siaj, M.; Larachi, F. *Chem. Eng. Process.* **2010**, *49*, 313−322.
(138) Ahnfeldt, T.; Guillou, N.; Gunzelmann, D.; Margiolaki, I.; Loiseau, T.; Férey, G.; Senker, J.; Stock, N. *Angew. Chem., Int. Ed.* **2009**, *48*, 5163−5166.
(139) Cao, L.; Lv, F.; Liu, Y.; Wang, W.; Huo, Y.; Fu, X.; Sun, R.; Lu, Z. *Chem. Commun.* **2015**, *51*, 4364−4367.
(140) Chiou, J. S.; Paul, D. R. *J. Appl. Polym. Sci.* **1987**, *34*, 1037−1056.
(141) Min, K. E.; Paul, D. R. *J. Polym. Sci., Part B: Polym. Phys.* **1988**, *26*, 1021−1033.
(142) Llewellyn, P. L.; Bourrelly, S.; Serre, C.; Vimont, A.; Daturi, M.; Hamon, L.; De Weireld, G.; Chang, J.-S.; Hong, D.-Y.; Kyu Hwang, Y.; Hwa Jhung, S.; Férey, G. *Langmuir* **2008**, *24*, 7245−7250.
(143) Xin, Q.; Ouyang, J.; Liu, T.; Li, Z.; Li, Z.; Liu, Y.; Wang, S.; Wu, H.; Jiang, Z.; Cao, X. *ACS Appl. Mater. Interfaces* **2015**, *7*, 1065−1077.
(144) Yan, Q.; Lin, Y.; Kong, C.; Chen, L. *Chem. Commun.* **2013**, *49*, 6873−6875.
(145) Hwang, Y. K.; Hong, D.-Y.; Chang, J.-S.; Jhung, S. H.; Seo, Y.-K.; Kim, J.; Vimont, A.; Daturi, M.; Serre, C.; Férey, G. *Angew. Chem., Int. Ed.* **2008**, *47*, 4144−4148.
(146) Hong, D.-Y.; Hwang, Y. K.; Serre, C.; Férey, G.; Chang, J.-S. *Adv. Funct. Mater.* **2009**, *19*, 1537−1552.
(147) Chui, S. S.-Y.; Lo, S. M.-F.; Charmant, J. P. H.; Orpen, A. G.; Williams, I. D. *Science* **1999**, *283*, 1148−1150.
(148) Taylor-Pashow, K. M. L.; Rocca, J. D.; Xie, Z.; Tran, S.; Lin, W. *J. Am. Chem. Soc.* **2009**, *131*, 14261−14263.
(149) Serre, C.; Millange, F.; Thouvenot, C.; Noguès, M.; Marsolier, G.; Louër, D.; Férey, G. *J. Am. Chem. Soc.* **2002**, *124*, 13519−13526.
(150) Millange, F.; Serre, C.; Guillou, N.; Férey, G.; Walton, R. I. *Angew. Chem., Int. Ed.* **2008**, *47*, 4100−4105.
(151) DeCoste, J. B.; Denny, M. S., Jr.; Peterson, G. W.; Mahle, J. J.; Cohen, S. M. *Chem. Sci.* **2016**, *7*, 2711−2716.
(152) DeCoste, J. B.; Peterson, G. W.; Schindler, B. J.; Killops, K. L.; Browe, M. A.; Mahle, J. J. *J. Mater. Chem. A* **2013**, *1*, 11922−11932.
(153) Zhang, Z.; Nguyen, H. T. H.; Miller, S. A.; Cohen, S. M. *Angew. Chem., Int. Ed.* **2015**, *54*, 6152−6157.
(154) Zhang, Z.; Nguyen, H. T. H.; Miller, S. A.; Ploskonka, A. M.; DeCoste, J. B.; Cohen, S. M. *J. Am. Chem. Soc.* **2016**, *138*, 920−925.
(155) Li, H.; Eddaoudi, M.; O'Keeffe, M.; Yaghi, O. M. *Nature* **1999**, *402*, 276−279.
(156) Tranchemontagne, D. J.; Hunt, J. R.; Yaghi, O. M. *Tetrahedron* **2008**, *64*, 8553−8557.
(157) Eddaoudi, M.; Kim, J.; Rosi, N.; Vodak, D.; Wachter, J.; O'Keeffe, M.; Yaghi, O. M. *Science* **2002**, *295*, 469−472.
(158) Allen, C. A.; Boissonnault, J. A.; Cirera, J.; Gulland, R.; Paesani, F.; Cohen, S. M. *Chem. Commun.* **2013**, *49*, 3200−3202.
(159) Allen, C. A.; Cohen, S. M. *Inorg. Chem.* **2014**, *53*, 7014−7019.
(160) Saha, D.; Bao, Z.; Jia, F.; Deng, S. *Environ. Sci. Technol.* **2010**, *44*, 1820−1826.
(161) Perez, E. V.; Balkus, K. J., Jr; Ferraris, J. P.; Musselman, I. H. *J. Membr. Sci.* **2009**, *328*, 165−173.
(162) Nugent, P.; Belmabkhout, Y.; Burd, S. D.; Cairns, A. J.; Luebke, R.; Forrest, K.; Pham, T.; Ma, S.; Space, B.; Wojtas, L.; Eddaoudi, M.; Zaworotko, M. J. *Nature* **2013**, *495*, 80−84.
(163) Henke, S.; Schneemann, A.; Kapoor, S.; Winter, R.; Fischer, R. A. *J. Mater. Chem.* **2012**, *22*, 909−918.
(164) Henke, S.; Fischer, R. A. *J. Am. Chem. Soc.* **2011**, *133*, 2064−2067.
(165) Henke, S.; Schneemann, A.; Wütscher, A.; Fischer, R. A. *J. Am. Chem. Soc.* **2012**, *134*, 9464−9474.
(166) Alaerts, L.; Maes, M.; Giebeler, L.; Jacobs, P. A.; Martens, J. A.; Denayer, J. F. M.; Kirschhock, C. E. A.; De Vos, D. E. *J. Am. Chem. Soc.* **2008**, *130*, 14170−14178.
(167) Millange, F.; Guillou, N.; Walton, R. I.; Greneche, J.-M.; Margiolaki, I.; Ferey, G. *Chem. Commun.* **2008**, 4732−4734.
(168) Basu, S.; Cano-Odena, A.; Vankelecom, I. F. J. *Sep. Purif. Technol.* **2011**, *81*, 31−40.
(169) Rodenas, T.; van Dalen, M.; García-Pérez, E.; Serra-Crespo, P.; Zornoza, B.; Kapteijn, F.; Gascon, J. *Adv. Funct. Mater.* **2014**, *24*, 249−256.
(170) Bhattacharya, A.; Misra, B. N. *Prog. Polym. Sci.* **2004**, *29*, 767−814.
(171) Tien-Binh, N.; Vinh-Thang, H.; Chen, X. Y.; Rodrigue, D.; Kaliaguine, S. *J. Mater. Chem. A* **2015**, *3*, 15202−15213.
(172) Ahmadi Feijani, E.; Mahdavi, H.; Tavasoli, A. *Chem. Eng. Res. Des.* **2015**, *96*, 87−102.
(173) Ahmadi Feijani, E.; Tavasoli, A.; Mahdavi, H. *Ind. Eng. Chem. Res.* **2015**, *54*, 12124−12134.
(174) Cai, W.; Lee, T.; Lee, M.; Cho, W.; Han, D.-Y.; Choi, N.; Yip, A. C. K.; Choi, J. *J. Am. Chem. Soc.* **2014**, *136*, 7961−7971.
(175) Li, T.; Pan, Y.; Peinemann, K.-V.; Lai, Z. *J. Membr. Sci.* **2013**, *425−426*, 235−242.
(176) Rezakazemi, M.; Ebadi Amooghin, A.; Montazer-Rahmati, M. M.; Ismail, A. F.; Matsuura, T. *Prog. Polym. Sci.* **2014**, *39*, 817−861.
(177) Ding, Z.-D.; Chi, Z.; Gu, W.-X.; Gu, S.-M.; Liu, J.-H.; Wang, H.-J. *Carbohydr. Polym.* **2012**, *89*, 7−16.
(178) Santos, E.; Rodríguez-Fernández, E.; Casado-Coterillo, C.; Irabien, Á. *Int. J. Chem. React. Eng.* **2016**, *14*, 713−718.
(179) Casado-Coterillo, C.; Fernandez-Barquin, A.; Zornoza, B.; Télez, C.; Coronas, J.; Irabien, A. *RSC Adv.* **2015**, *5*, 102350−102361.
(180) Zhou, F.; Koros, W. J. *Polymer* **2006**, *47*, 280−288.
(181) Bos, A.; Pünt, I. G. M.; Wessling, M.; Strathmann, H. *Sep. Purif. Technol.* **1998**, *14*, 27−39.
(182) Mahdi, E. M.; Tan, J.-C. *J. Membr. Sci.* **2016**, *498*, 276−290.
(183) Song, Q.; Nataraj, S. K.; Roussenova, M. V.; Tan, J. C.; Hughes, D. J.; Li, W.; Bourgoin, P.; Alam, M. A.; Cheetham, A. K.; Al-Muhtaseb, S. A.; Sivaniah, E. *Energy Environ. Sci.* **2012**, *5*, 8359−8369.
(184) Aroon, M. A.; Ismail, A. F.; Matsuura, T.; Montazer-Rahmati, M. M. *Sep. Purif. Technol.* **2010**, *75*, 229−242.
(185) Carne, A.; Carbonell, C.; Imaz, I.; Maspoch, D. *Chem. Soc. Rev.* **2011**, *40*, 291−305.
(186) Tanaka, D.; Henke, A.; Albrecht, K.; Moeller, M.; Nakagawa, K.; Kitagawa, S.; Groll, J. *Nat. Chem.* **2010**, *2*, 410−416.
(187) Tanaka, S.; Fujita, K.; Miyake, Y.; Miyamoto, M.; Hasegawa, Y.; Makino, T.; Van der Perre, S.; Cousin Saint Remi, J.; Van Assche, T.; Baron, G. V.; Denayer, J. F. M. *J. Phys. Chem. C* **2015**, *119*, 28430−28439.
(188) Yang, J.-M.; Liu, Q.; Sun, W.-Y. *J. Solid State Chem.* **2014**, *218*, 50−55.
(189) Stavitski, E.; Goesten, M.; Juan-Alcañiz, J.; Martinez-Joaristi, A.; Serra-Crespo, P.; Petukhov, A. V.; Gascon, J.; Kapteijn, F. *Angew. Chem., Int. Ed.* **2011**, *50*, 9624−9628.
(190) Taddei, M.; Dau, P. V.; Cohen, S. M.; Ranocchiari, M.; van Bokhoven, J. A.; Costantino, F.; Sabatini, S.; Vivani, R. *Dalton Trans.* **2015**, *44*, 14019−14026.

DOI: 10.1021/acs.cgd.7b00595
Cryst. Growth Des. 2017, 17, 4467−4488

(191) Liu, B.; Zou, R.-Q.; Zhong, R.-Q.; Han, S.; Shioyama, H.; Yamada, T.; Maruta, G.; Takeda, S.; Xu, Q. *Microporous Mesoporous Mater.* **2008**, *111*, 470−477.
(192) Ziaee, A.; Chovan, D.; Lusi, M.; Perry, J. J.; Zaworotko, M. J.; Tofail, S. A. M. *Cryst. Growth Des.* **2016**, *16*, 3890−3897.
(193) Uemura, K.; Maeda, A.; Maji, T. K.; Kanoo, P.; Kita, H. *Eur. J. Inorg. Chem.* **2009**, *2009*, 2329−2337.
(194) Shekhah, O.; Belmabkhout, Y.; Chen, Z.; Guillerm, V.; Cairns, A.; Adil, K.; Eddaoudi, M. *Nat. Commun.* **2014**, *5*, 4228.
(195) Gong, H.; Nguyen, T. H.; Wang, R.; Bae, T.-H. *J. Membr. Sci.* **2015**, *495*, 169−175.
(196) Hu, Z.; Nalaparaju, A.; Peng, Y.; Jiang, J.; Zhao, D. *Inorg. Chem.* **2016**, *55*, 1134−1141.
(197) Hu, Z.; Kang, Z.; Qian, Y.; Peng, Y.; Wang, X.; Chi, C.; Zhao, D. *Ind. Eng. Chem. Res.* **2016**, *55*, 7933.
(198) Ricco, R.; Pfeiffer, C.; Sumida, K.; Sumby, C. J.; Falcaro, P.; Furukawa, S.; Champness, N. R.; Doonan, C. J. *CrystEngComm* **2016**, *18*, 6532−6542.
(199) Seoane, B.; Castellanos, S.; Dikhtiarenko, A.; Kapteijn, F.; Gascon, J. *Coord. Chem. Rev.* **2016**, *307* (Part 2), 147−187.
(200) Sabetghadam, A.; Seoane, B.; Keskin, D.; Duim, N.; Rodenas, T.; Shahid, S.; Sorribas, S.; Guillouzer, C. L.; Clet, G.; Téllez, C.; Daturi, M.; Coronas, J.; Kapteijn, F.; Gascon, J. *Adv. Funct. Mater.* **2016**, *26*, 3154−3163.
(201) Kang, Z.; Peng, Y.; Hu, Z.; Qian, Y.; Chi, C.; Yeo, L. Y.; Tee, L.; Zhao, D. *J. Mater. Chem. A* **2015**, *3*, 20801−20810.
(202) Rodenas, T.; Luz, I.; Prieto, G.; Seoane, B.; Miro, H.; Corma, A.; Kapteijn, F.; Llabrés i Xamena, F. X.; Gascon, J. *Nat. Mater.* **2015**, *14*, 48−55.
(203) Sanchez, C.; Julian, B.; Belleville, P.; Popall, M. *J. Mater. Chem.* **2005**, *15*, 3559−3592.
(204) Shahid, S.; Nijmeijer, K.; Nehache, S.; Vankelecom, I.; Deratani, A.; Quemener, D. *J. Membr. Sci.* **2015**, *492*, 21−31.
(205) Shahid, S.; Nijmeijer, K. *J. Membr. Sci.* **2014**, *470*, 166−177.
(206) Hwang, S.; Chi, W. S.; Lee, S. J.; Im, S. H.; Kim, J. H.; Kim, J. *J. Membr. Sci.* **2015**, *480*, 11−19.
(207) Sánchez-Laínez, J.; Zornoza, B.; Friebe, S.; Caro, J.; Cao, S.; Sabetghadam, A.; Seoane, B.; Gascon, J.; Kapteijn, F.; Le Guillouzer, C.; Clet, G.; Daturi, M.; Téllez, C.; Coronas, J. *J. Membr. Sci.* **2016**, *515*, 45−53.
(208) Brown, A. J.; Brunelli, N. A.; Eum, K.; Rashidi, F.; Johnson, J. R.; Koros, W. J.; Jones, C. W.; Nair, S. *Science* **2014**, *345*, 72−75.
(209) Biswal, B. P.; Bhaskar, A.; Banerjee, R.; Kharul, U. K. *Nanoscale* **2015**, *7*, 7291−7298.
(210) Cacho-Bailo, F.; Caro, G.; Etxeberria-Benavides, M.; Karvan, O.; Téllez, C.; Coronas, J. *Chem. Commun.* **2015**, *51*, 11283−11285.
(211) Cacho-Bailo, F.; Catalán-Aguirre, S.; Etxeberría-Benavides, M.; Karvan, O.; Sebastian, V.; Téllez, C.; Coronas, J. *J. Membr. Sci.* **2015**, *476*, 277−285.
(212) Cacho-Bailo, F.; Caro, G.; Etxeberria-Benavides, M.; Karvan, O.; Téllez, C.; Coronas, J. *RSC Adv.* **2016**, *6*, 5881−5889.
(213) Férey, G. *Eur. J. Inorg. Chem.* **2016**, *2016*, 4275−4277.

DOI: 10.1021/acs.cgd.7b00595
Cryst. Growth Des. 2017, 17, 4467−4488